A new multidimensional-type reconstruction and limiting procedure for unstructured (cell-centered) FVs solving hyperbolic conservation laws

Argiris I. Delis

&

Ioannis K. Nikolos (TUC)

Department of Sciences-Division of Mathematics
Technical University of Crete (TUC), Chania, Greece

Introduction & Motivation

➜ High-order Finite Volume (FV) schemes on unstructured meshes is, probably, the most used approach for approximating CL.

Introduction & Motivation

- ➜ High-order Finite Volume (FV) schemes on unstructured meshes is, probably, the most used approach for approximating CL.
- ➜ Mainly two basic formulations of the FV method: the cell-centered (**CCFV**) and the node-centered (**NCFV**), one on triangular grids.

Introduction & Motivation

- High-order Finite Volume (FV) schemes on unstructured meshes is, probably, the most used approach for approximating CL.
- Mainly two basic formulations of the FV method: the cell-centered (**CCFV**) and the node-centered (**NCFV**), one on triangular grids.
- A lot of current-day 2D CFD codes rely, almost exclusively, on formal second order accurate FV schemes following the MUSCL-type framework achieved in two stages: **(a)** solution reconstruction stage from cell-average values **(b)** use of an (approximate) Riemann solver.

Introduction & Motivation

- ➜ High-order Finite Volume (FV) schemes on unstructured meshes is, probably, the most used approach for approximating CL.
- ➜ Mainly two basic formulations of the FV method: the cell-centered (**CCFV**) and the node-centered (**NCFV**), one on triangular grids.
- ➜ A lot of current-day 2D CFD codes rely, almost exclusively, on formal second order accurate FV schemes following the MUSCL-type framework achieved in two stages: **(a)** solution reconstruction stage from cell-average values **(b)** use of an (approximate) Riemann solver.
- ➜ High-order reconstruction can capture complex flow structures but may entail non-physical oscillations near discontinuities which may lead to wrong solutions or serious stability and convergence problems.

Introduction & Motivation

- High-order Finite Volume (FV) schemes on unstructured meshes is, probably, the most used approach for approximating CL.
- Mainly two basic formulations of the FV method: the cell-centered (**CCFV**) and the node-centered (**NCFV**), one on triangular grids.
- A lot of current-day 2D CFD codes rely, almost exclusively, on formal second order accurate FV schemes following the MUSCL-type framework achieved in two stages: **(a)** solution reconstruction stage from cell-average values **(b)** use of an (approximate) Riemann solver.
- High-order reconstruction can capture complex flow structures but may entail non-physical oscillations near discontinuities which may lead to wrong solutions or serious stability and convergence problems.
- **Multidimensional limiting**, based on the satisfaction of the Maximum Principle (for monotonic reconstruction), Barth & Jespersen (1989), Venkatakrishnan (1993-95), Batten et al. (1996), Hubbard (1999), Berger et al. (2005), Park et al. (2010-12).

➜ However, need the **use of non-differentiable functions** like the $\min$ and $\max$, and limit at the cost of multiple constrained, data dependent, **minimization problems** at each computational cell and time step.

- However, need the **use of non-differentiable functions** like the $\min$ and $\max$, and limit at the cost of multiple constrained, data dependent, **minimization problems** at each computational cell and time step.
- Although current reconstruction and limiting approaches have enjoyed relative success, there is **no consensus** on the optimal strategy to fulfill a high-level of accuracy and robustness.

- However, need the **use of non-differentiable functions** like the $\min$ and $\max$, and limit at the cost of multiple constrained, data dependent, **minimization problems** at each computational cell and time step.
- Although current reconstruction and limiting approaches have enjoyed relative success, there is **no consensus** on the optimal strategy to fulfill a high-level of accuracy and robustness.
- May have to use different approaches for the CCFV and NCFV formulations e.g in poor connected grids.

- However, need the **use of non-differentiable functions** like the $\min$ and $\max$, and limit at the cost of multiple constrained, data dependent, **minimization problems** at each computational cell and time step.
- Although current reconstruction and limiting approaches have enjoyed relative success, there is **no consensus** on the optimal strategy to fulfill a high-level of accuracy and robustness.
- May have to use different approaches for the CCFV and NCFV formulations e.g in poor connected grids.
- **Grid topology** can be an issue, especially for **distorted**, **stretched** and **hybrid meshes**, as well as **boundary treatment**. Different behavior may exhibited on different meshes.

- However, need the **use of non-differentiable functions** like the $\min$ and $\max$, and limit at the cost of multiple constrained, data dependent, **minimization problems** at each computational cell and time step.

- Although current reconstruction and limiting approaches have enjoyed relative success, there is **no consensus** on the optimal strategy to fulfill a high-level of accuracy and robustness.

- May have to use different approaches for the CCFV and NCFV formulations e.g in poor connected grids.

- **Grid topology** can be an issue, especially for **distorted**, **stretched** and **hybrid meshes**, as well as **boundary treatment**. Different behavior may exhibited on different meshes.

- May need to compare the CCFV approach with the NCFV (median dual or centroid dual) one in a unified framework, e.g. Delis et al. (2011).

Overview

➜ Different grids and grid terminology used (mostly) in this work

Overview

- Different grids and grid terminology used (mostly) in this work
- Finite Volumes on triangles: the cell-centered (CCFV) and node-centered (NCFV) approach, **in a unified framework**.

Overview

- Different grids and grid terminology used (mostly) in this work
- Finite Volumes on triangles: the cell-centered (CCFV) and node-centered (NCFV) approach, **in a unified framework**.
- Use of MUSCL-type linear reconstruction, utilizing the Green-Gauss gradient computations and classical approximate Riemann solvers (Roe's and HLLC) and Runge-Kutta temporal discretization.

Overview

- Different grids and grid terminology used (mostly) in this work
- Finite Volumes on triangles: the cell-centered (CCFV) and node-centered (NCFV) approach, **in a unified framework**.
- Use of MUSCL-type linear reconstruction, utilizing the Green-Gauss gradient computations and classical approximate Riemann solvers (Roe's and HLLC) and Runge-Kutta temporal discretization.
- Mesh geometrical considerations and the **proposed linear reconstruction** and **edge-based limiting**.

Overview

- Different grids and grid terminology used (mostly) in this work
- Finite Volumes on triangles: the cell-centered (CCFV) and node-centered (NCFV) approach, **in a unified framework**.
- Use of MUSCL-type linear reconstruction, utilizing the Green-Gauss gradient computations and classical approximate Riemann solvers (Roe´s and HLLC) and Runge-Kutta temporal discretization.
- Mesh geometrical considerations and the **proposed linear reconstruction** and **edge-based limiting**.
- Numerical tests and reults for the Non-linear Shallow Water Equations (using a well-balanced FV scheme).

Overview

- ➜ Different grids and grid terminology used (mostly) in this work
- ➜ Finite Volumes on triangles: the cell-centered (CCFV) and node-centered (NCFV) approach, **in a unified framework**.
- ➜ Use of MUSCL-type linear reconstruction, utilizing the Green-Gauss gradient computations and classical approximate Riemann solvers (Roe´s and HLLC) and Runge-Kutta temporal discretization.
- ➜ Mesh geometrical considerations and the **proposed linear reconstruction** and **edge-based limiting**.
- ➜ Numerical tests and reults for the Non-linear Shallow Water Equations (using a well-balanced FV scheme).
- ➜ Numerical tests and results for the (inviscid) Euler equations.

Overview

- ➜ Different grids and grid terminology used (mostly) in this work
- ➜ Finite Volumes on triangles: the cell-centered (CCFV) and node-centered (NCFV) approach, **in a unified framework**.
- ➜ Use of MUSCL-type linear reconstruction, utilizing the Green-Gauss gradient computations and classical approximate Riemann solvers (Roe´s and HLLC) and Runge-Kutta temporal discretization.
- ➜ Mesh geometrical considerations and the **proposed linear reconstruction** and **edge-based limiting**.
- ➜ Numerical tests and reults for the Non-linear Shallow Water Equations (using a well-balanced FV scheme).
- ➜ Numerical tests and results for the (inviscid) Euler equations.
- ➜ Comparisons with (truly) multidimensional limiters.

Overview

➜ Different grids and grid terminology used (mostly) in this work

➜ Finite Volumes on triangles: the cell-centered (CCFV) and node-centered (NCFV) approach, **in a unified framework**.

➜ Use of MUSCL-type linear reconstruction, utilizing the Green-Gauss gradient computations and classical approximate Riemann solvers (Roe´s and HLLC) and Runge-Kutta temporal discretization.

➜ Mesh geometrical considerations and the **proposed linear reconstruction** and **edge-based limiting**.

➜ Numerical tests and reults for the Non-linear Shallow Water Equations (using a well-balanced FV scheme).

➜ Numerical tests and results for the (inviscid) Euler equations.

➜ Comparisons with (truly) multidimensional limiters.

Grids & Terminology

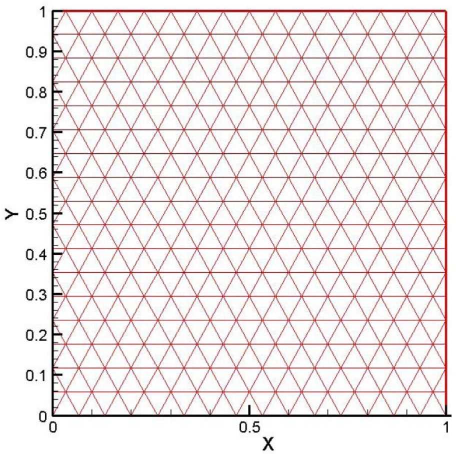

(a) **Equilateral (Type-I)**

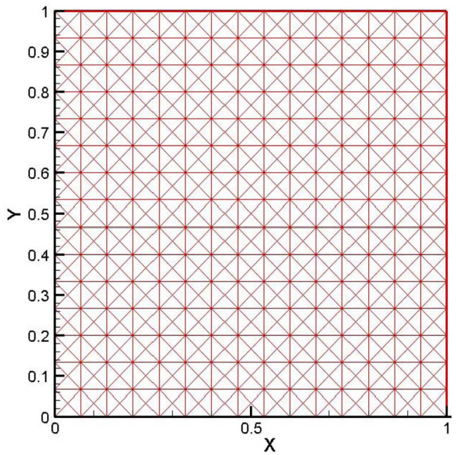

(b) **Orthogonal (Type-II)**

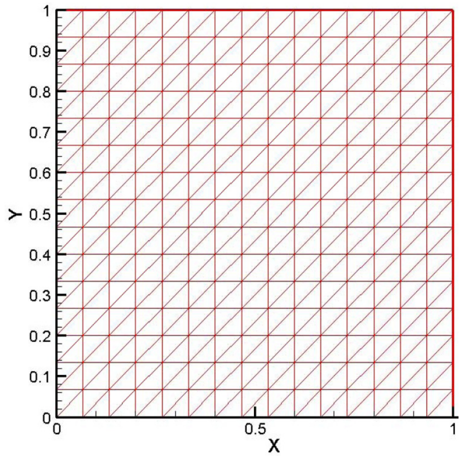

(c) **Orthogonal (Type-III)**

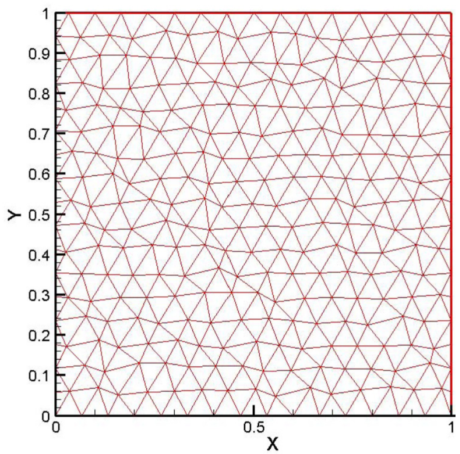

(d) **Distorted (Type-IV)**

Grids & Terminology

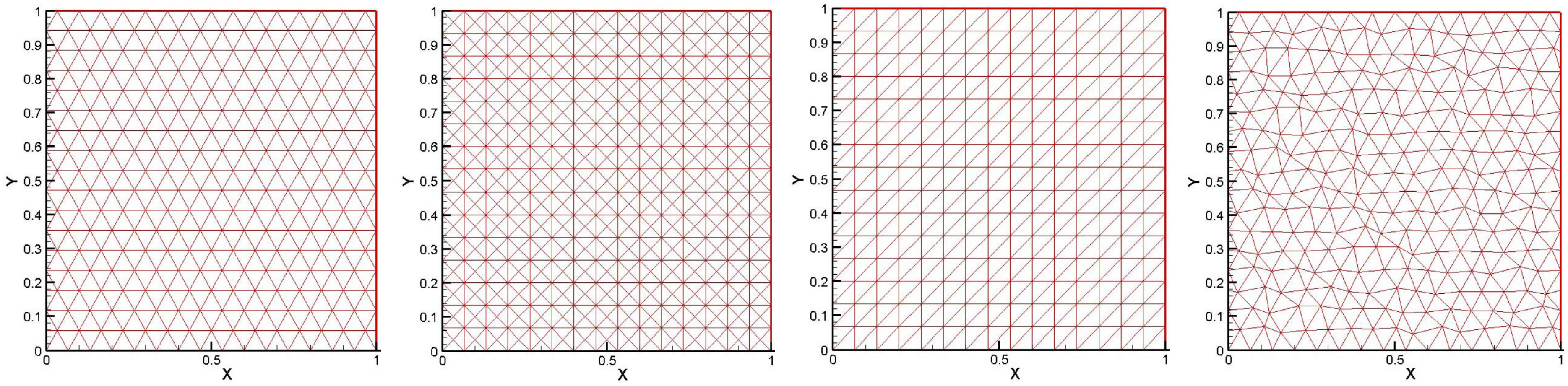

(a) **Equilateral (Type-I)** (b) **Orthogonal (Type-II)** (c) **Orthogonal (Type-III)** (d) **Distorted (Type-IV)**

➜ Major requirement: to enable meaningful asymptotic order of convergence use **consistently refined grids,** i.e. for $N =$ degrees of freedom, the characteristic length $h_N = \sqrt{(L_x \times L_y)/N}$

Grids & Terminology

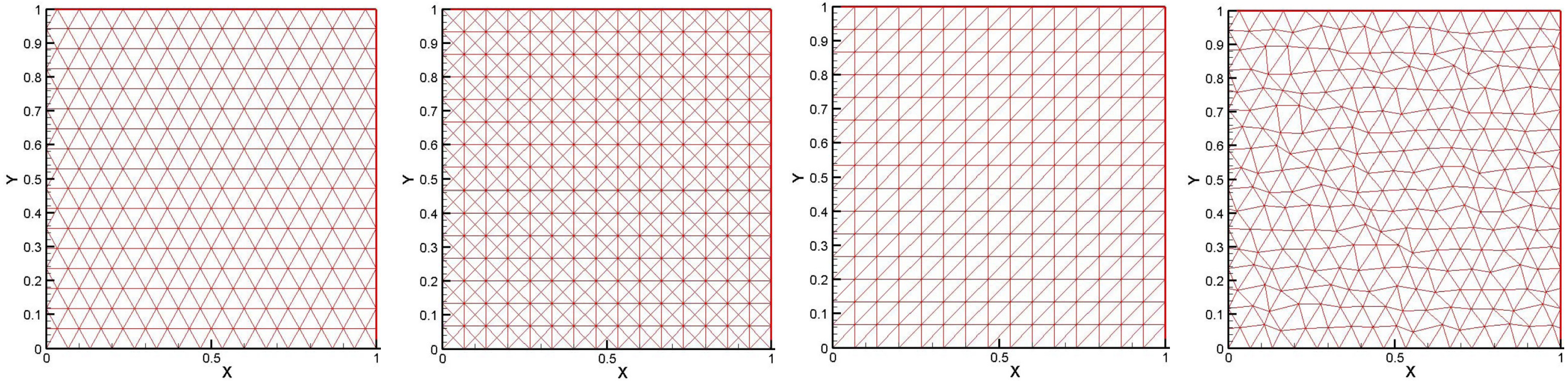

(a) **Equilateral (Type-I)** (b) **Orthogonal (Type-II)** (c) **Orthogonal (Type-III)** (d) **Distorted (Type-IV)**

➜ Major requirement: to enable meaningful asymptotic order of convergence use **consistently refined grids,** i.e. for $N =$ degrees of freedom, the characteristic length $h_N = \sqrt{(L_x \times L_y)/N}$

➜ For fair comparisons, also between the CCFV and NCFV approach, need to derive **equivalent meshes**, based on the degrees of freedom N

Grids & Terminology

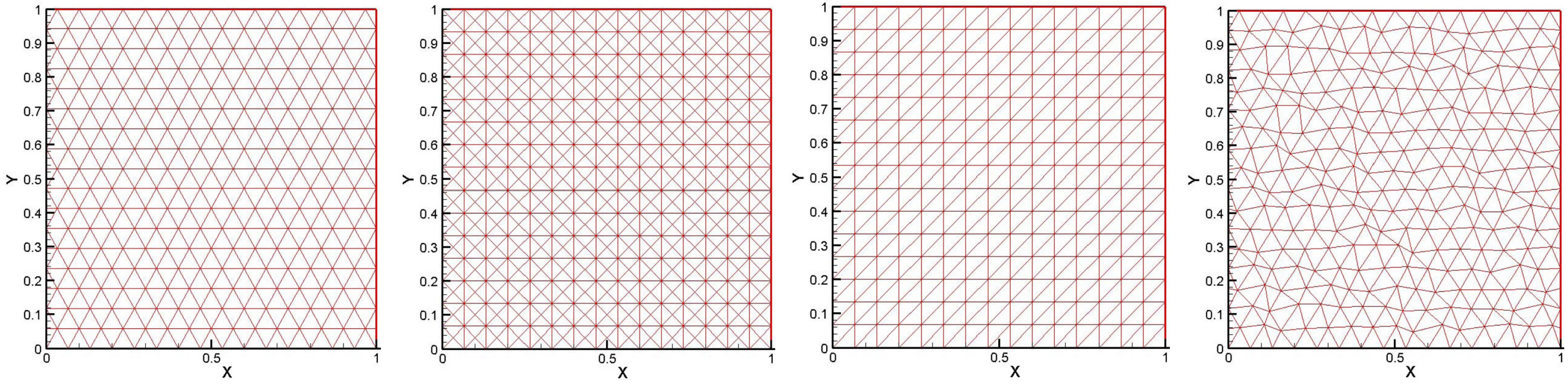

(a) **Equilateral (Type-I)** (b) **Orthogonal (Type-II)** (c) **Orthogonal (Type-III)** (d) **Distorted (Type-IV)**

- Major requirement: to enable meaningful asymptotic order of convergence use **consistently refined grids,** i.e. for $N =$ degrees of freedom, the characteristic length $h_N = \sqrt{(L_x \times L_y)/N}$

- For fair comparisons, also between the CCFV and NCFV approach, need to derive **equivalent meshes**, based on the degrees of freedom N

- Term **edge** will refer to the line connecting neighboring data points (locations of discrete solutions) and **faces** are the FV cell boundaries

FV discretization schemes on triangles: CCFV approach

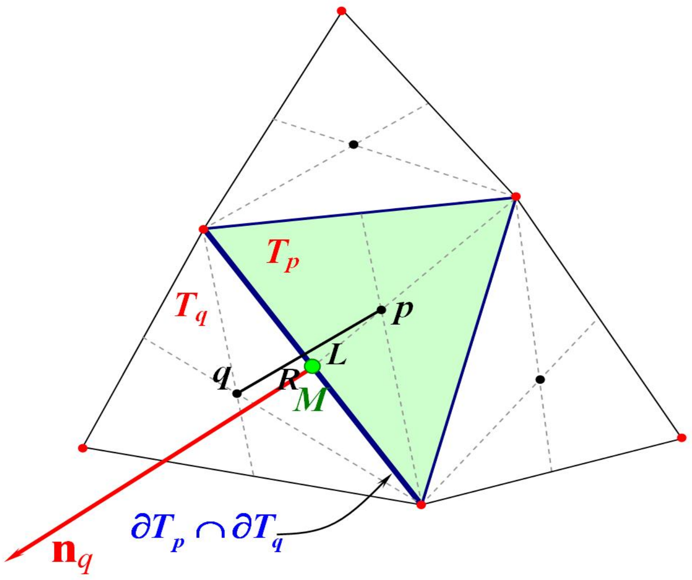

$$\iint_{T_p} \frac{\partial \mathbf{W}}{\partial t} dxdy + \oint_{\partial T_p} \left(\mathbf{F}\widetilde{n}_{q_x} + \mathbf{G}\widetilde{n}_{q_y} \right) dl = \iint_{T_p} \mathcal{L}\, dxdy$$

$$\frac{\partial \mathbf{W}_p}{\partial t}|T_p| = \sum_{q \in K(p)} \mathbf{\Phi}_q + \iint_{T_p} \mathcal{L} d\Omega,$$

with the usual one point quadrature at M,

$\mathbf{\Phi}_q =$ Numerical flux function,

evaluated at $\mathbf{W}^L$ and $\mathbf{W}^R$ **reconstructed** values.

FV discretization schemes on triangles: CCFV approach

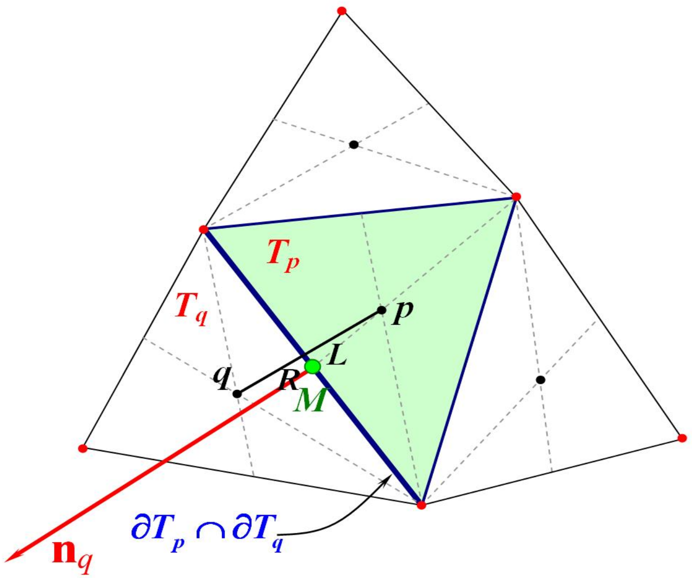

$$\iint_{T_p} \frac{\partial \mathbf{W}}{\partial t} dxdy + \oint_{\partial T_p} \left(\mathbf{F}\widetilde{n}_{q_x} + \mathbf{G}\widetilde{n}_{q_y} \right) dl = \iint_{T_p} \mathcal{L}\, dxdy$$

$$\frac{\partial \mathbf{W}_p}{\partial t} |T_p| = \sum_{q \in K(p)} \mathbf{\Phi}_q + \iint_{T_p} \mathcal{L} d\Omega,$$

with the usual one point quadrature at M,

$\mathbf{\Phi}_q =$ Numerical flux function,

evaluated at $\mathbf{W}^L$ and $\mathbf{W}^R$ **reconstructed** values.

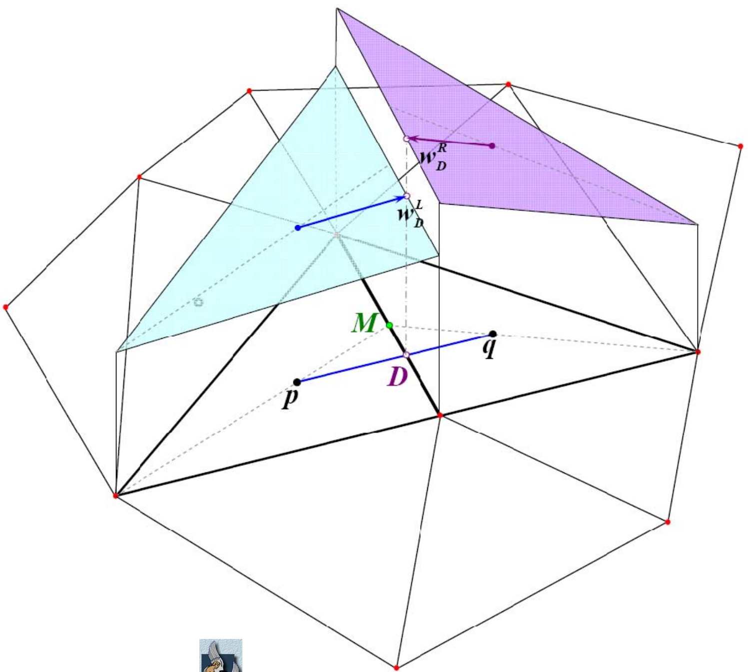

Linear reconstruction for the CCFV scheme

- **Naive** reconstruction (at point D)

$$\begin{aligned} (w_{i,p})_D^L &= w_{i,p} + \mathbf{r}_{pD} \cdot \nabla w_{i,p}; \\ (w_{i,q})_D^R &= w_{i,q} - \mathbf{r}_{Dq} \cdot \nabla w_{i,q}, \end{aligned}$$

FV discretization schemes on triangles: CCFV approach

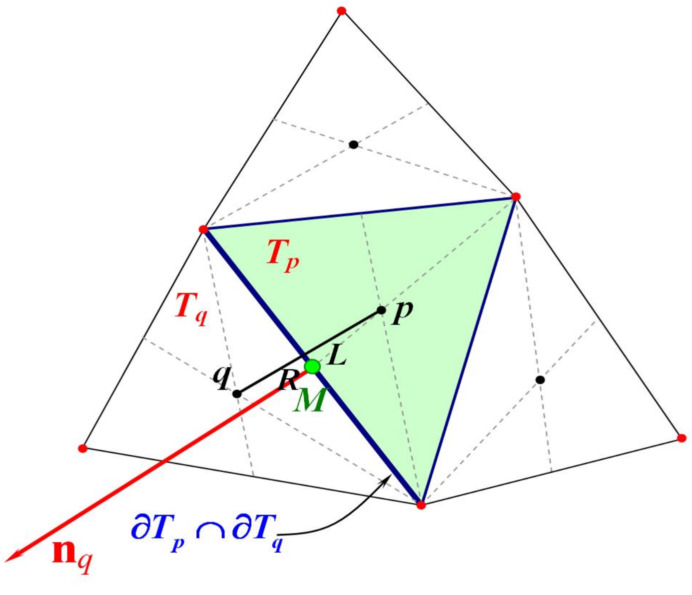

$$\iint_{T_p} \frac{\partial \mathbf{W}}{\partial t} dx dy + \oint_{\partial T_p} \left(\mathbf{F} \widetilde{n}_{q_x} + \mathbf{G} \widetilde{n}_{q_y} \right) dl = \iint_{T_p} \mathcal{L} \, dx dy$$

$$\frac{\partial \mathbf{W}_p}{\partial t} |T_p| = \sum_{q \in K(p)} \mathbf{\Phi}_q + \iint_{T_p} \mathcal{L} d\Omega,$$

with the usual one point quadrature at M,

$\mathbf{\Phi}_q =$ Numerical flux function,

evaluated at $\mathbf{W}^L$ and $\mathbf{W}^R$ **reconstructed** values.

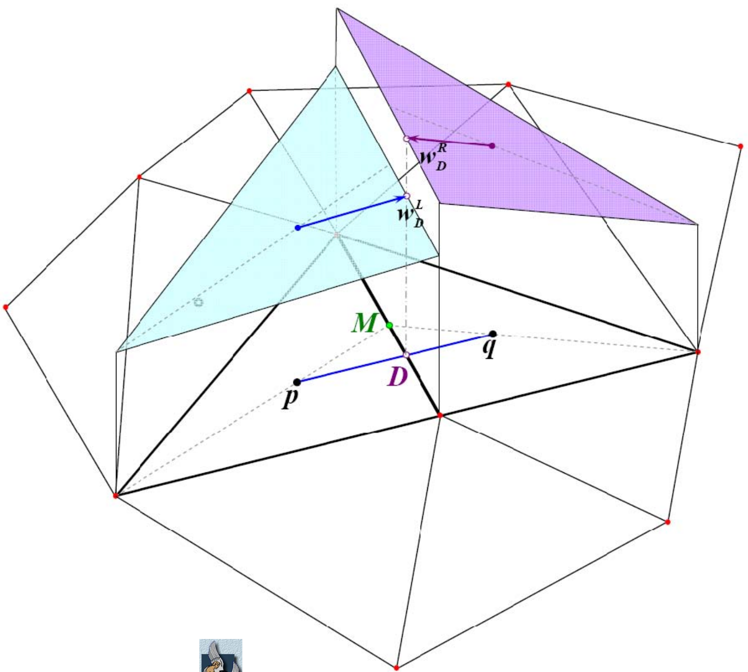

Linear reconstruction for the CCFV scheme

- **Naive** reconstruction (at point D)

$$\begin{aligned} (w_{i,p})_D^L &= w_{i,p} + \mathbf{r}_{pD} \cdot \nabla w_{i,p}; \\ (w_{i,q})_D^R &= w_{i,q} - \mathbf{r}_{Dq} \cdot \nabla w_{i,q}, \end{aligned}$$

- Monotonicity in the reconstruction will be enforced by using **edge-based** slope limiters.

FV discretization schemes on triangles: CCFV approach

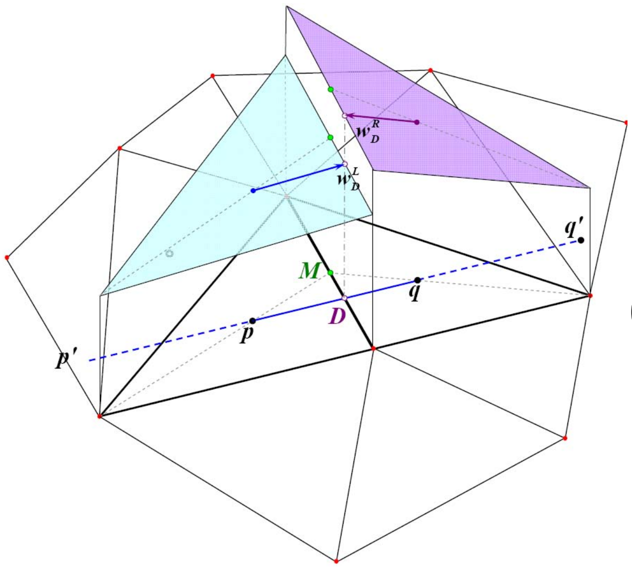

- **Limited** naive reconstruction at point D

$$(w_{i,q})_D^R = w_{i,q} - \frac{||\mathbf{r}_{Dq}||}{||\mathbf{r}_{pq}||} \text{LIM}\left((\nabla w_{i,q})^{\mathsf{U}} \cdot \mathbf{r}_{pq}, (\nabla w_{i,q})^{\mathsf{C}} \cdot \mathbf{r}_{pq} \right);$$

$$(w_{i,p})_D^L = w_{i,p} + \frac{||\mathbf{r}_{pD}||}{||\mathbf{r}_{pq}||} \text{LIM}\left((\nabla w_{i,p})^{\mathsf{U}} \cdot \mathbf{r}_{pq}, (\nabla w_{i,p})^{\mathsf{C}} \cdot \mathbf{r}_{pq} \right),$$

where $(\nabla w_{i,q})^{\mathsf{C}} \cdot \mathbf{r}_{pq} = w_{i,q} - w_{i,p}$ and $(\nabla w_{i,p})^{\mathsf{U}} = 2\,(\nabla w_{i,p}) - (\nabla w_{i,p})^{\mathsf{C}}$.

FV discretization schemes on triangles: CCFV approach

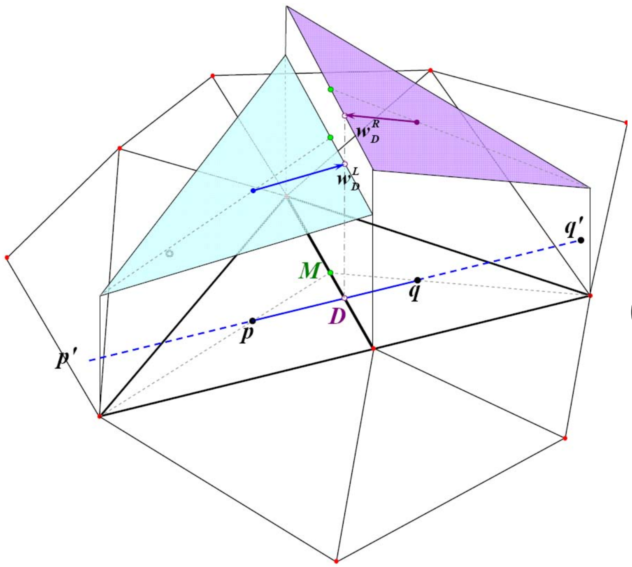

- **Limited** naive reconstruction at point D

$$(w_{i,q})_D^R = w_{i,q} - \frac{||\mathbf{r}_{Dq}||}{||\mathbf{r}_{pq}||} \mathsf{LIM}\left((\nabla w_{i,q})^{\mathsf{u}} \cdot \mathbf{r}_{pq}, (\nabla w_{i,q})^{\mathsf{c}} \cdot \mathbf{r}_{pq} \right) ;$$

$$(w_{i,p})_D^L = w_{i,p} + \frac{||\mathbf{r}_{pD}||}{||\mathbf{r}_{pq}||} \mathsf{LIM}\left((\nabla w_{i,p})^{\mathsf{u}} \cdot \mathbf{r}_{pq}, (\nabla w_{i,p})^{\mathsf{c}} \cdot \mathbf{r}_{pq} \right) ,$$

where $(\nabla w_{i,q})^{\mathsf{c}} \cdot \mathbf{r}_{pq} = w_{i,q} - w_{i,p}$ and $(\nabla w_{i,p})^{\mathsf{u}} = 2\,(\nabla w_{i,p}) - (\nabla w_{i,p})^{\mathsf{c}}$.

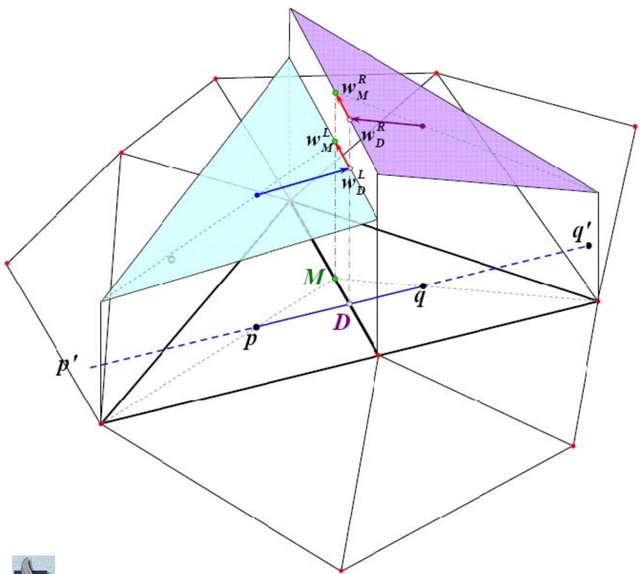

- **Directionaly corrected** reconstruction at M

$$(w_{i,p})_{\mathrm{M}}^L = (w_{i,p})_D^L + \mathbf{r}_{DM} \cdot (\nabla w_{i,p}) ,$$

$$(w_{i,q})_{\mathrm{M}}^R = (w_{i,q})_D^R + \mathbf{r}_{DM} \cdot (\nabla w_{i,q}) .$$

FV discretization schemes on triangles: CCFV approach

- **Limited directionally corrected** reconstruction at point $\mathbf{M}$, for $(w_{i,p})^{L}_{\mathbf{M}}$

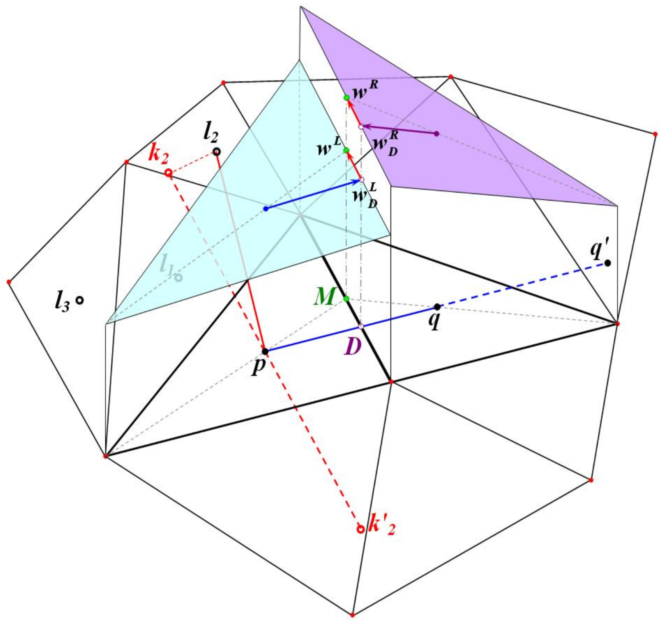

- Identify triangles T_{l_j}, with indices $l_j, j = 1, 2, 3$, that have a common vertex with T_p in the direction of $\overline{DM}$.

FV discretization schemes on triangles: CCFV approach

- **Limited directionally corrected** reconstruction at point $\mathbf{M}$, for $(w_{i,p})^L_{\mathbf{M}}$

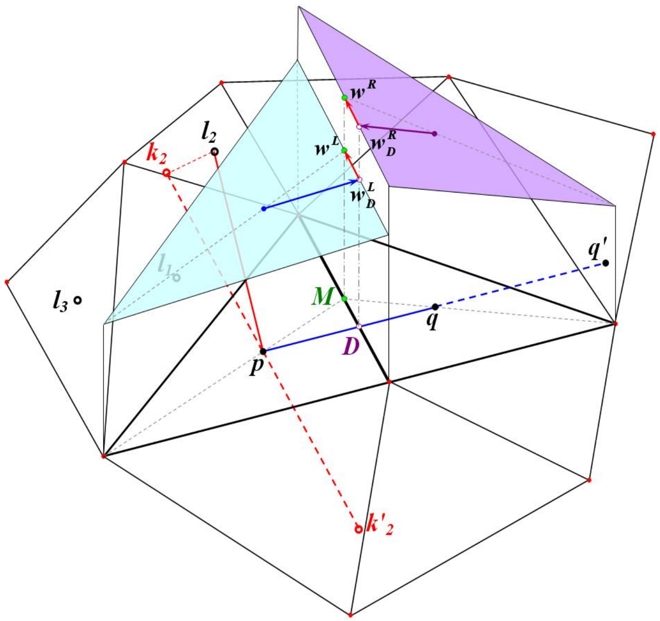

- Identify triangles T_{l_j}, with indices $l_j, j = 1, 2, 3$, that have a common vertex with T_p in the direction of $\overline{DM}$.
- Choose as a reference triangle that for which $\overline{pl_j}$ has the smallest angle with $\overline{DM}$

FV discretization schemes on triangles: CCFV approach

- **Limited directionally corrected** reconstruction at point $\mathbf{M}$, for $(w_{i,p})^L_{\mathbf{M}}$

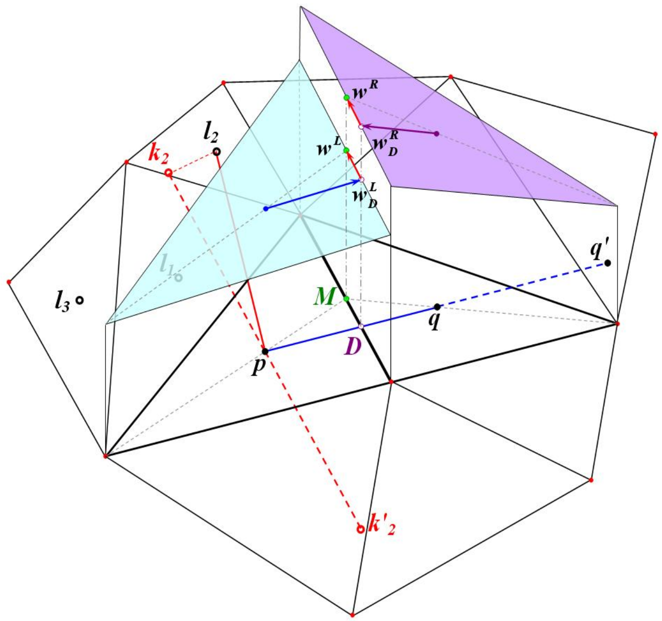

- Identify triangles T_{l_j}, with indices $l_j, j = 1, 2, 3$, that have a common vertex with T_p in the direction of $\overline{DM}$.
- Choose as a reference triangle that for which $\overline{pl_j}$ has the smallest angle with $\overline{DM}$
- Project its cell center in the direction of $\overline{DM}$ (i.e. $\overline{pk_2}$)

FV discretization schemes on triangles: CCFV approach

- **Limited directionally corrected** reconstruction at point $\mathbf{M}$, for $(w_{i,p})^L_{\mathbf{M}}$

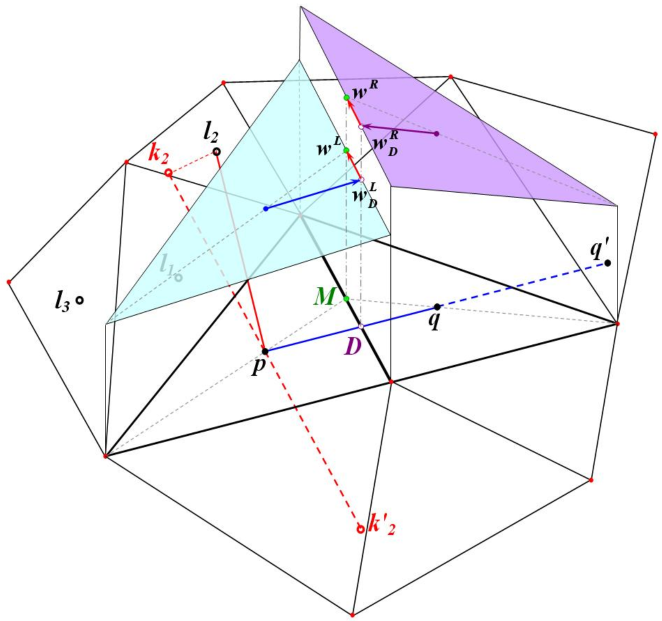

- Identify triangles T_{l_j}, with indices $l_j, j = 1, 2, 3$, that have a common vertex with T_p in the direction of $\overline{DM}$.
- Choose as a reference triangle that for which $\overline{pl_j}$ has the smallest angle with $\overline{DM}$
- Project its cell center in the direction of $\overline{DM}$ (i.e. $\overline{pk_2}$)
- The extrapolated value at k_2 can be given as

$$w_{i,k2} = w_{i,l_2} + \mathbf{r}_{l_2k_2} \cdot (\nabla w_{i,l_2})$$

FV discretization schemes on triangles: CCFV approach

- **Limited directionally corrected** reconstruction at point $\mathbf{M}$, for $(w_{i,p})^L_{\mathbf{M}}$

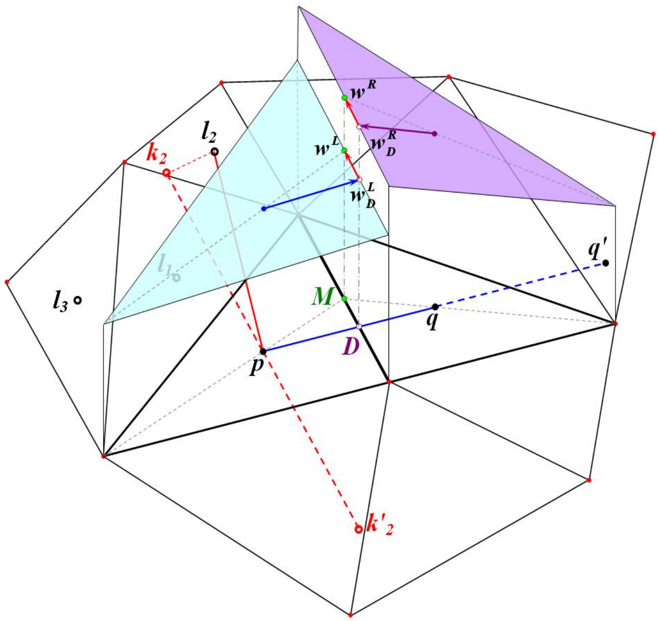

- Identify triangles T_{l_j}, with indices $l_j, j = 1, 2, 3$, that have a common vertex with T_p in the direction of $\overline{DM}$.
- Choose as a reference triangle that for which $\overline{pl_j}$ has the smallest angle with $\overline{DM}$
- Project its cell center in the direction of $\overline{DM}$ (i.e. $\overline{pk_2}$)
- The extrapolated value at k_2 can be given as

$$w_{i,k2} = w_{i,l_2} + \mathbf{r}_{l_2 k_2} \cdot (\nabla w_{i,l_2})$$

- The local central reference gradient is defined now as

$$(\nabla w_{i,p})^{\mathsf{C}} \cdot \mathbf{r}_{pk_2} = w_{i,k_2} - w_{i,p}$$

FV discretization schemes on triangles: CCFV approach

- **Limited directionally corrected** reconstruction at point $\mathbf{M}$, for $(w_{i,p})^L_{\mathbf{M}}$

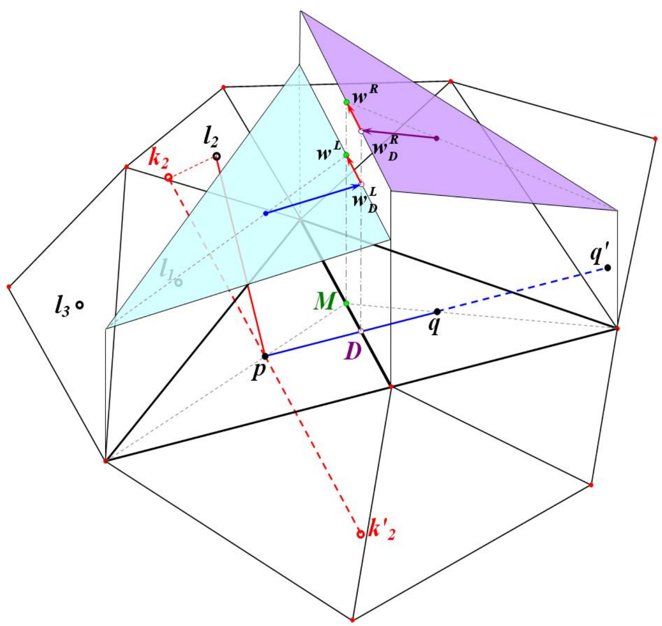

- Identify triangles T_{l_j}, with indices $l_j, j = 1, 2, 3$, that have a common vertex with T_p in the direction of $\overline{DM}$.
- Choose as a reference triangle that for which $\overline{pl_j}$ has the smallest angle with $\overline{DM}$
- Project its cell center in the direction of $\overline{DM}$ (i.e. $\overline{pk_2}$)
- The extrapolated value at k_2 can be given as

$$w_{i,k2} = w_{i,l_2} + \mathbf{r}_{l_2k_2} \cdot (\nabla w_{i,l_2})$$

- The local central reference gradient is defined now as

$$(\nabla w_{i,p})^{\mathsf{c}} \cdot \mathbf{r}_{pk_2} = w_{i,k_2} - w_{i,p}$$

- Compute the upwind gradient $w_{i,p} - w_{i,k'_2}$ to get

$$(\nabla w_{i,p})^{\mathsf{u}} = 2\,(\nabla w_{i,p}) - (\nabla w_{i,p})^{\mathsf{c}}$$

FV discretization schemes on triangles: CCFV approach

- **Limited directionally corrected** reconstruction at point $\mathbf{M}$, for $(w_{i,p})^L_{\mathbf{M}}$

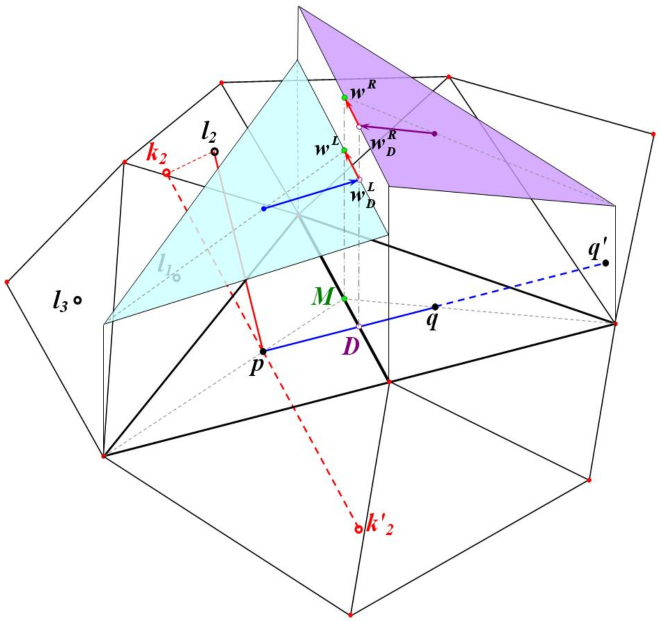

- Identify triangles T_{l_j}, with indices $l_j, j = 1, 2, 3$, that have a common vertex with T_p in the direction of $\overline{DM}$.
- Choose as a reference triangle that for which $\overline{pl_j}$ has the smallest angle with $\overline{DM}$
- Project its cell center in the direction of $\overline{DM}$ (i.e. $\overline{pk_2}$)
- The extrapolated value at k_2 can be given as

$$w_{i,k2} = w_{i,l_2} + \mathbf{r}_{l_2 k_2} \cdot (\nabla w_{i,l_2})$$

- The local central reference gradient is defined now as

$$(\nabla w_{i,p})^{\mathsf{c}} \cdot \mathbf{r}_{pk_2} = w_{i,k_2} - w_{i,p}$$

- Compute the upwind gradient $w_{i,p} - w_{i,k'_2}$ to get

$$(\nabla w_{i,p})^{\mathsf{u}} = 2\,(\nabla w_{i,p}) - (\nabla w_{i,p})^{\mathsf{c}}$$

FV discretization schemes on triangles: CCFV approach

Finally the, now corrected and limited, left and right reconstructed values at the flux integration point $\mathbf{M}$ are given as

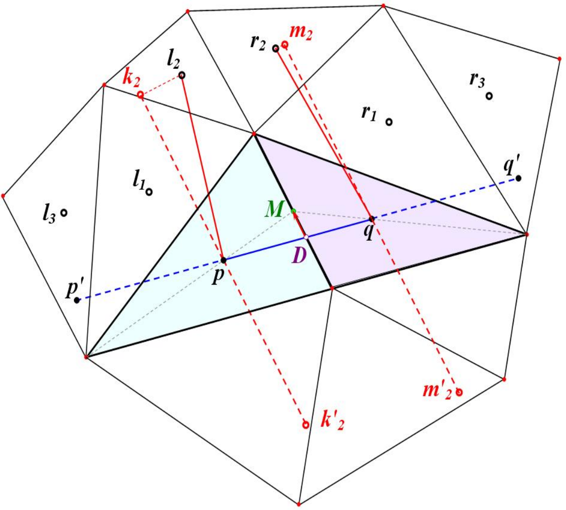

$$(w_{i,p})^L_{\mathbf{M}} = (w_{i,p})^L_D + \frac{||\mathbf{r}_{DM}||}{||\mathbf{r}_{pk_2}||}\text{LIM}\left((\nabla w_{i,p})^{\text{u}} \cdot \mathbf{r}_{pk_2}, (\nabla w_{i,p})^{\text{c}} \cdot \mathbf{r}_{pk_2}\right);$$

$$(w_{i,q})^R_{\mathbf{M}} = (w_{i,q})^R_D + \frac{||\mathbf{r}_{DM}||}{||\mathbf{r}_{qm_2}||}\text{LIM}\left((\nabla w_{i,q})^{\text{u}} \cdot \mathbf{r}_{qm_2}, (\nabla w_{i,q})^{\text{c}} \cdot \mathbf{r}_{qm_2}\right).$$

FV discretization schemes on triangles: CCFV approach

Finally the, now corrected and limited, left and right reconstructed values at the flux integration point $\mathbf{M}$ are given as

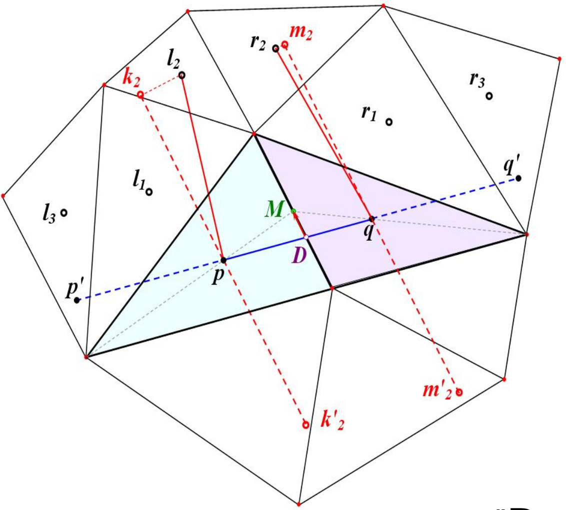

$$(w_{i,p})^L_{\mathbf{M}} = (w_{i,p})^L_D + \frac{||\mathbf{r}_{DM}||}{||\mathbf{r}_{pk_2}||}\text{LIM}\left((\nabla w_{i,p})^{\text{U}} \cdot \mathbf{r}_{pk_2}, (\nabla w_{i,p})^{\text{C}} \cdot \mathbf{r}_{pk_2}\right);$$

$$(w_{i,q})^R_{\mathbf{M}} = (w_{i,q})^R_D + \frac{||\mathbf{r}_{DM}||}{||\mathbf{r}_{qm_2}||}\text{LIM}\left((\nabla w_{i,q})^{\text{U}} \cdot \mathbf{r}_{qm_2}, (\nabla w_{i,q})^{\text{C}} \cdot \mathbf{r}_{qm_2}\right).$$

"Prototype" limiter function, the modified Van Albada-Van Leer limiter:

$$\text{LIM}(a,b) = \begin{cases} \dfrac{\left(a^2+e\right)b + \left(b^2+e\right)a}{a^2+b^2+2e} & \text{if } ab > 0, \\ 0 & \text{if } ab \le 0, \end{cases} \qquad 0 < e << 1$$

- Continuous differentiable (helps in achieving smooth transitions)
- Can achieve second-order accuracy in all usual norms

Green-Gauss (GG) gradient operators Barth & Jespersen (1989)

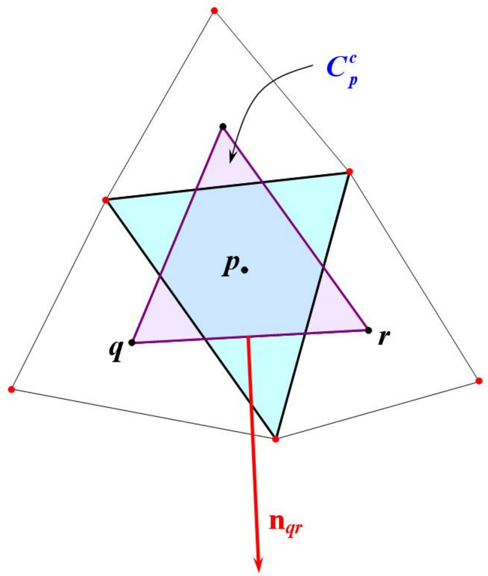

Three element (compact stencil) gradient

$$\nabla w_{i,p} = \frac{1}{|C_p^c|} \sum_{\substack{q,r \in K(p) \\ r \neq q}} \frac{1}{2}\Big(w_{i,q} + w_{i,r}\Big)\mathbf{n}_{qr}.$$

Green-Gauss (GG) gradient operators Barth & Jespersen (1989)

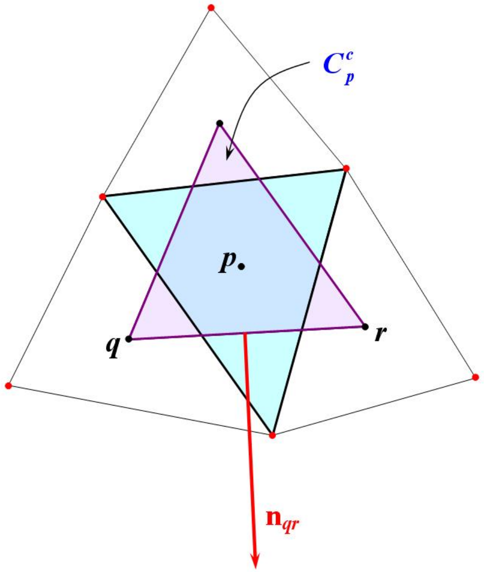

Three element (compact stencil) gradient

$$\nabla w_{i,p} = \frac{1}{|C_p^c|} \sum_{\substack{q,r \in K(p) \\ r \neq q}} \frac{1}{2}\Big(w_{i,q} + w_{i,r}\Big)\mathbf{n}_{qr}.$$

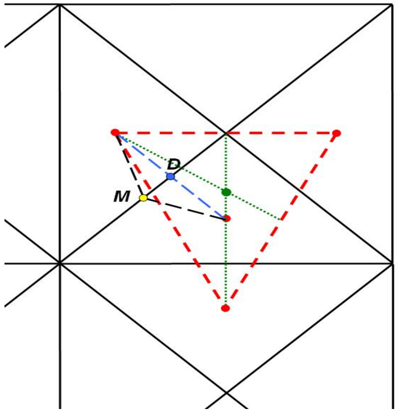

M may lay outside gradient's volume!

Green-Gauss (GG) gradient operators Barth & Jespersen (1989)

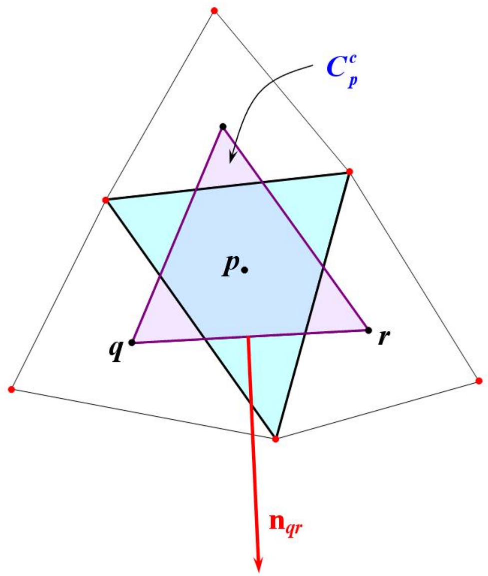

Three element (compact stencil) gradient

$$\nabla w_{i,p} = \frac{1}{|C_p^c|} \sum_{\substack{q,r \in K(p) \\ r \neq q}} \frac{1}{2}\Big(w_{i,q} + w_{i,r}\Big)\mathbf{n}_{qr}.$$

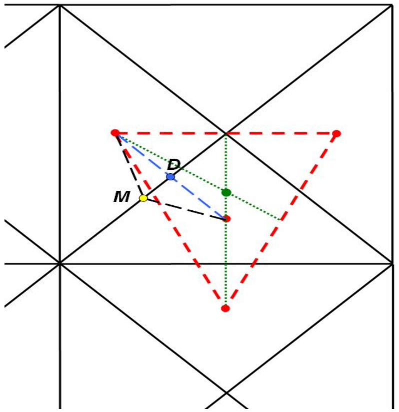

M may lay outside gradient's volume!

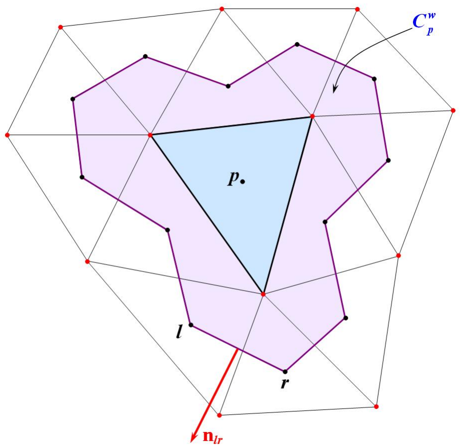

Extended element (wide stencil) gradient

$$\nabla w_{i,p} = \frac{1}{|C_p^w|} \sum_{\substack{l,r \in K'(p) \\ r \neq l}} \frac{1}{2}\Big(w_{i,l} + w_{i,r}\Big)\mathbf{n}_{lr}$$

Green-Gauss (GG) gradient operators Barth & Jespersen (1989)

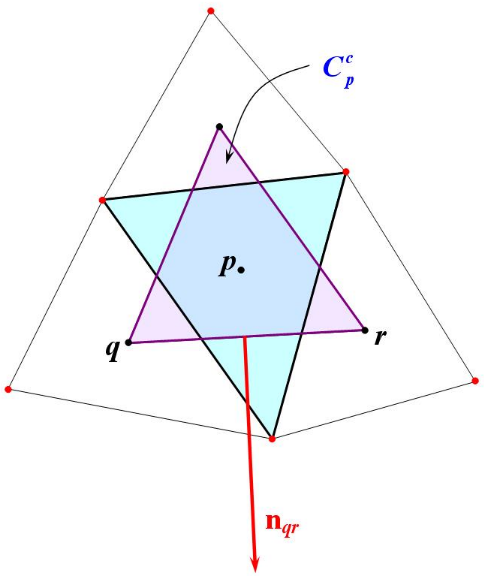

Three element (compact stencil) gradient

$$\nabla w_{i,p} = \frac{1}{|C_p^c|} \sum_{\substack{q,r \in K(p) \\ r \neq q}} \frac{1}{2}\Big(w_{i,q} + w_{i,r}\Big)\mathbf{n}_{qr}.$$

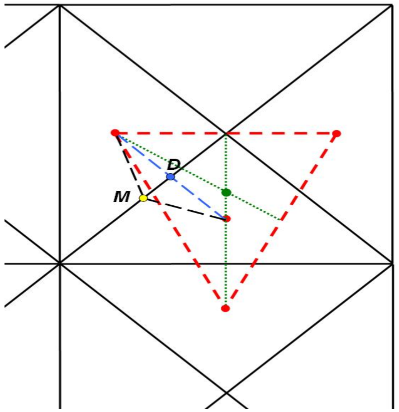

M may lay outside gradient's volume!

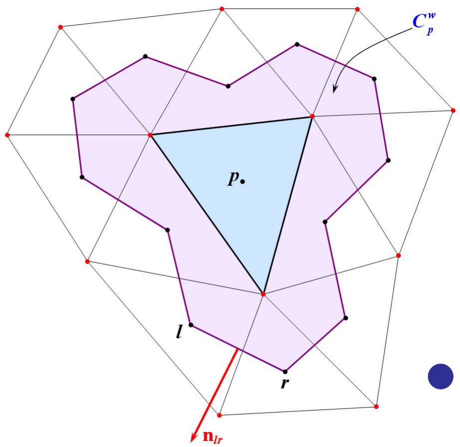

Extended element (wide stencil) gradient

$$\nabla w_{i,p} = \frac{1}{|C_p^w|} \sum_{\substack{l,r \in K'(p) \\ r \neq l}} \frac{1}{2}\Big(w_{i,l} + w_{i,r}\Big)\mathbf{n}_{lr}$$

- Satisfies the **good neighborhood** for Van Leer limiting (Swartz, 1999)

Typical behavior of the CCFV scheme at internal and boundary faces

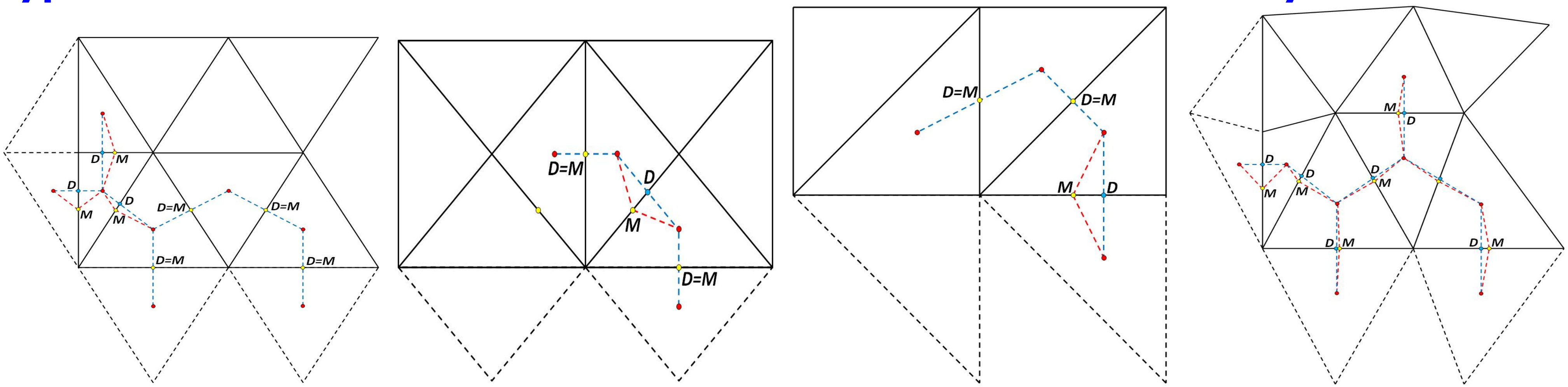

• In an ideal unstructured grid, variables are extrapolated at $\mathbf{M}$ which will coincide with D (intersection point of face $\partial T_q \cap \partial T_p$ and $\overline{pq}$).

Typical behavior of the CCFV scheme at internal and boundary faces

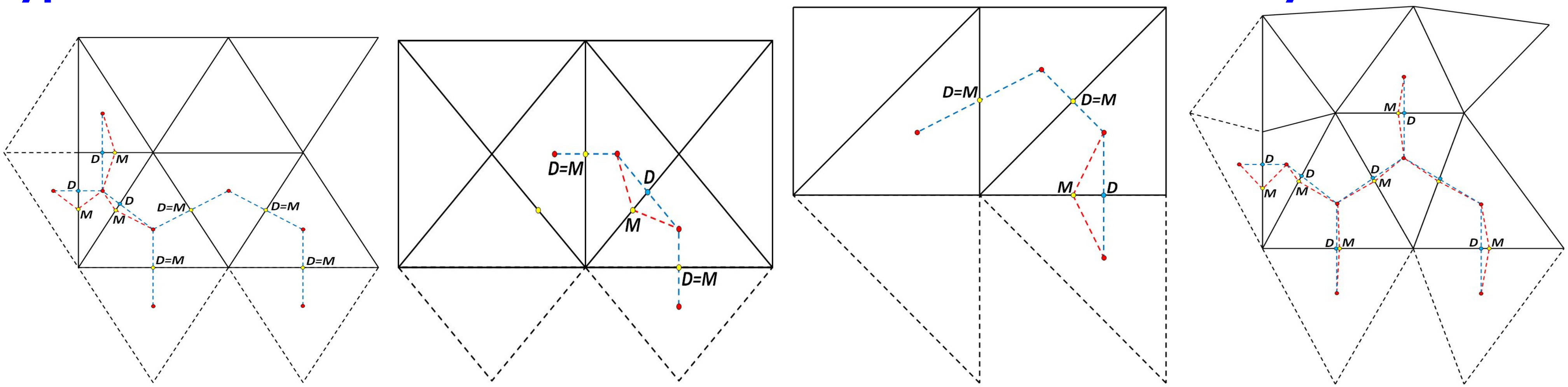

● In an ideal unstructured grid, variables are extrapolated at $\mathbf{M}$ which will coincide with D (intersection point of face $\partial T_q \cap \partial T_p$ and $\overline{pq}$).

● **Ghost cells** are used and the method of characteristics to enforce boundary conditions.

Typical behavior of the CCFV scheme at internal and boundary faces

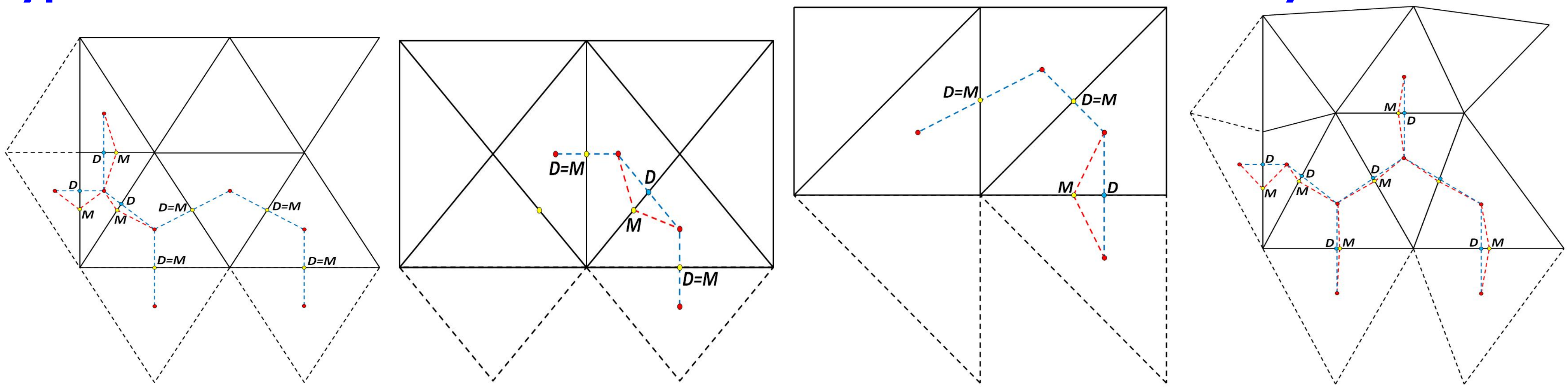

- In an ideal unstructured grid, variables are extrapolated at $\mathbf{M}$ which will coincide with D (intersection point of face $\partial T_q \cap \partial T_p$ and $\overline{pq}$).
- **Ghost cells** are used and the method of characteristics to enforce boundary conditions.
- There can be a **large distance** between $\mathbf{M}$ and D (also on boundary faces, where ghost cells are used).

Typical behavior of the CCFV scheme at internal and boundary faces

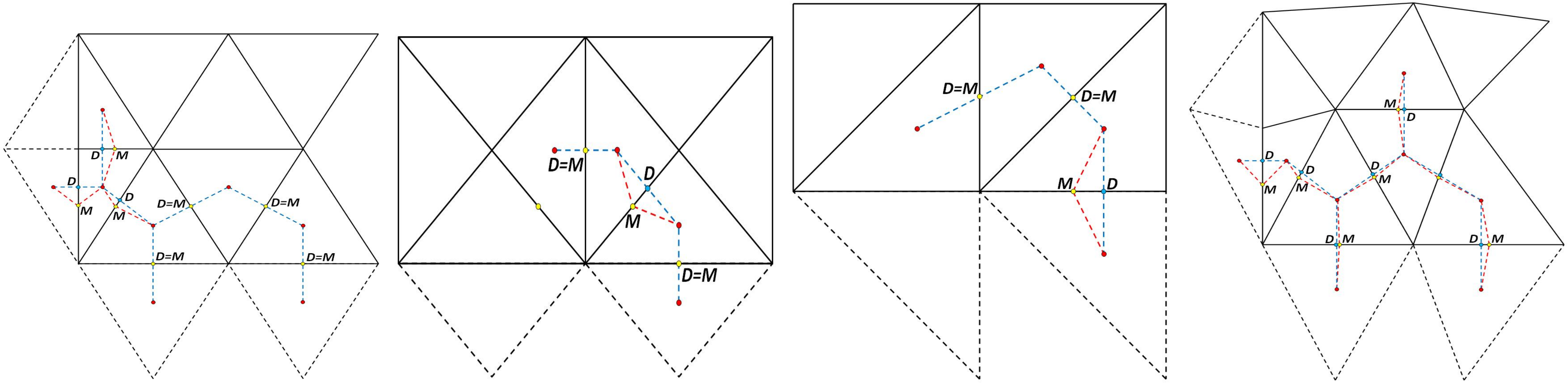

- In an ideal unstructured grid, variables are extrapolated at M which will coincide with D (intersection point of face $\partial T_q \cap \partial T_p$ and $\overline{pq}$).
- **Ghost cells** are used and the method of characteristics to enforce boundary conditions.
- There can be a **large distance** between M and D (also on boundary faces, where ghost cells are used).
- However, the compact stencil has to be used for the GG gradient computation at the boundary.

FV discretization schemes on triangles: NCFV approach

FV discretization schemes on triangles: NCFV approach

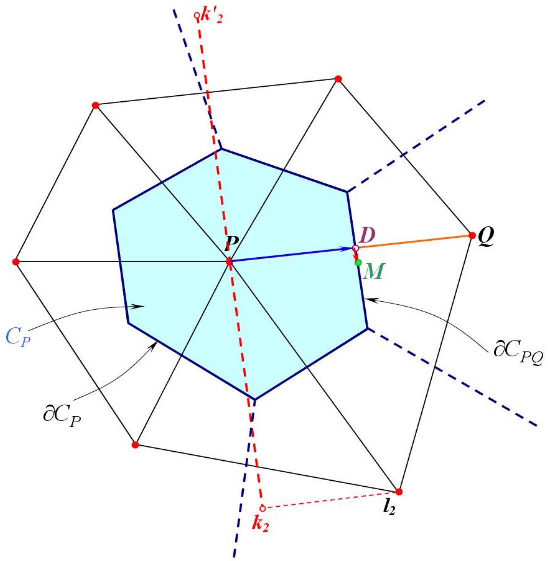

(e) **Centroid Dual**

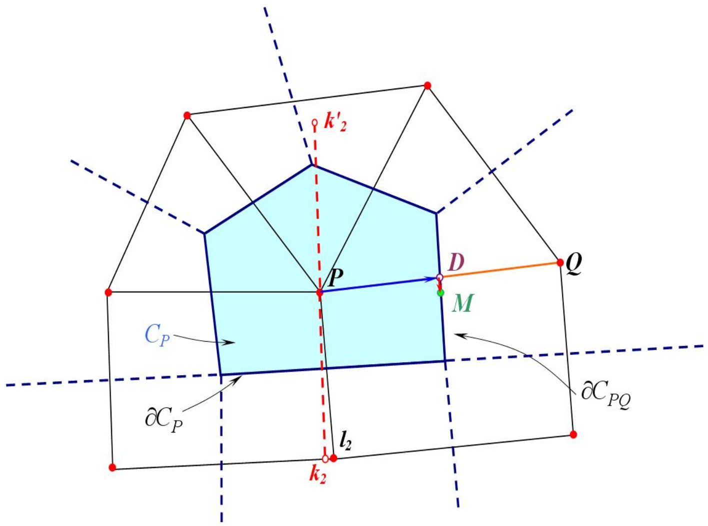

(f) **Hybrid mesh**

FV discretization schemes on triangles: NCFV approach

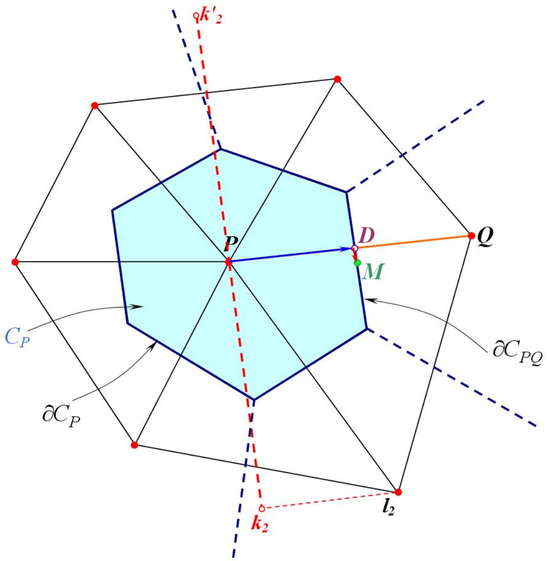

(e) **Centroid Dual**

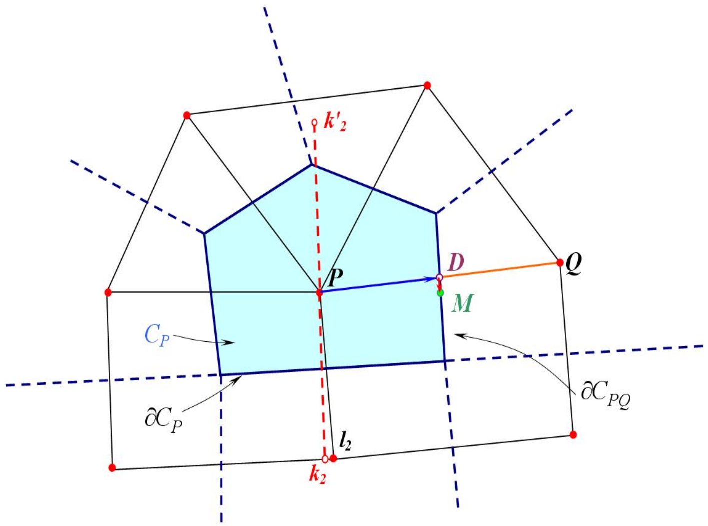

(f) **Hybrid mesh**

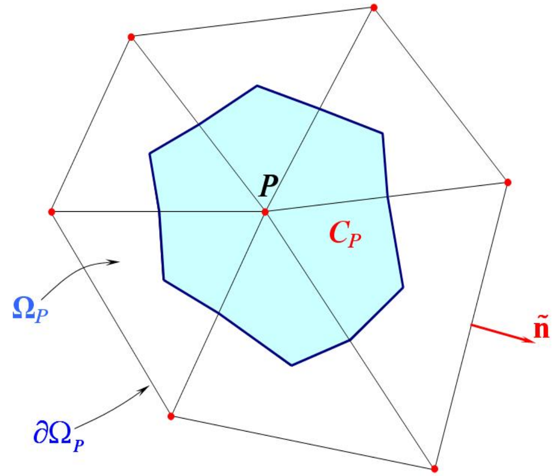

(g) **GG gradient stencil**

$$\frac{\partial \mathbf{W}_P}{\partial t}|C_P| + \sum_{Q\in K_P} \mathbf{\Phi}_{PQ} + \mathbf{\Phi}_{P,out} = \iint_{C_P} \mathcal{L}\, dxdy \quad \text{where}$$

$$\mathbf{\Phi}_{PQ} = \text{Numerical flux function} \quad \text{and} \quad \mathbf{\Phi}_{P,out} = \text{boundary flux}$$

evaluated again at $\mathbf{W}^L_{PQ}$ and $\mathbf{W}^R_{PQ}$ **reconstructed** values.

Numerical results and Comparisons I (Shallow Water Flows)

Scheme	Description
CCFVc1	Naive reconstruction (compact stencil gradient)
CCFVc2L	Limited directional correction (compact stencil gradient)
CCFVw1	Naive reconstruction (wide stencil gradient)
CCFVw2L	Limited directional correction (wide stencil gradient)
Unlimited	The basic CCFV scheme (linear MUSCL reconstruction, no limiting)
V-scheme	The CCFV scheme using Venkatakrishnan's V-limiter
MLPu2	The CCFV scheme using ML of Park et al, JCP, 2010

Numerical results and Comparisons I (Shallow Water Flows)

Scheme	Description
CCFVc1	Naive reconstruction (compact stencil gradient)
CCFVc2L	Limited directional correction (compact stencil gradient)
CCFVw1	Naive reconstruction (wide stencil gradient)
CCFVw2L	Limited directional correction (wide stencil gradient)
Unlimited	The basic CCFV scheme (linear MUSCL reconstruction, no limiting)
V-scheme	The CCFV scheme using Venkatakrishnan's V-limiter
MLPu2	The CCFV scheme using ML of Park et al, JCP, 2010

Ia **A traveling vortex solution** (with periodic boundary conditions)

Using Roe's Riemann solver

Numerical results and Comparisons I (Shallow Water Flows)

Scheme	Description
CCFVc1	Naive reconstruction (compact stencil gradient)
CCFVc2L	Limited directional correction (compact stencil gradient)
CCFVw1	Naive reconstruction (wide stencil gradient)
CCFVw2L	Limited directional correction (wide stencil gradient)
Unlimited	The basic CCFV scheme (linear MUSCL reconstruction, no limiting)
V-scheme	The CCFV scheme using Venkatakrishnan's V-limiter
MLPu2	The CCFV scheme using ML of Park et al, JCP, 2010

Ia **A traveling vortex solution** (with periodic boundary conditions)

Using Roe's Riemann solver

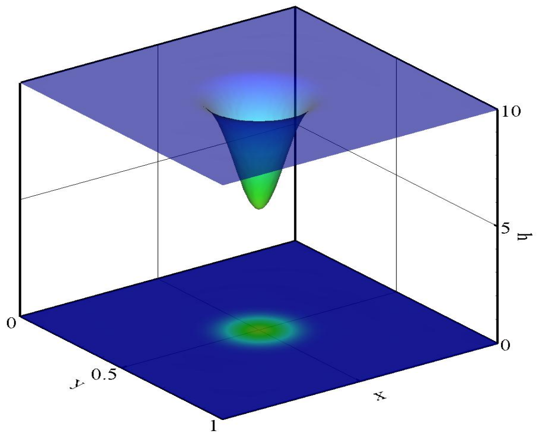

Numerical results and Comparisons I (Shallow Water Flows)

Scheme	Description
CCFVc1	Naive reconstruction (compact stencil gradient)
CCFVc2L	Limited directional correction (compact stencil gradient)
CCFVw1	Naive reconstruction (wide stencil gradient)
CCFVw2L	Limited directional correction (wide stencil gradient)
Unlimited	The basic CCFV scheme (linear MUSCL reconstruction, no limiting)
V-scheme	The CCFV scheme using Venkatakrishnan's V-limiter
MLPu2	The CCFV scheme using ML of Park et al, JCP, 2010

Ia **A traveling vortex solution** (with periodic boundary conditions)

Using Roe's Riemann solver

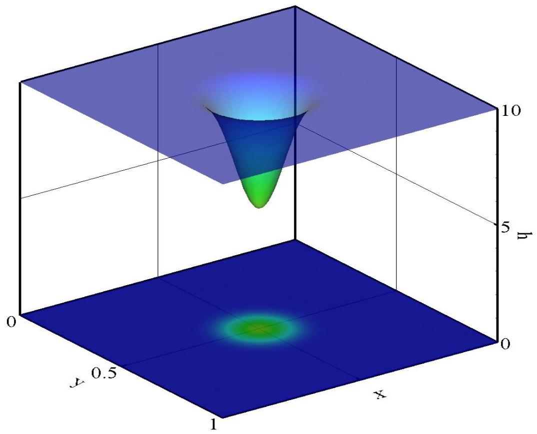

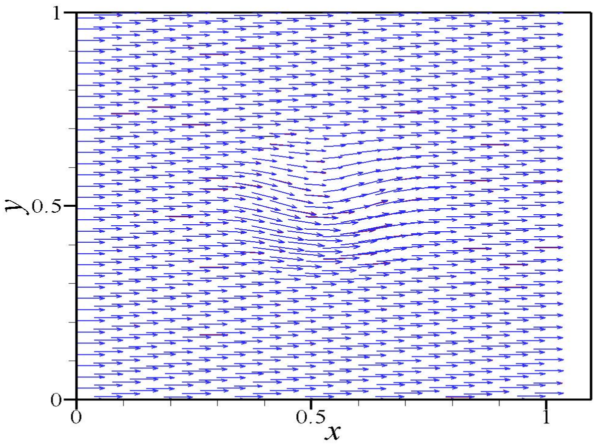

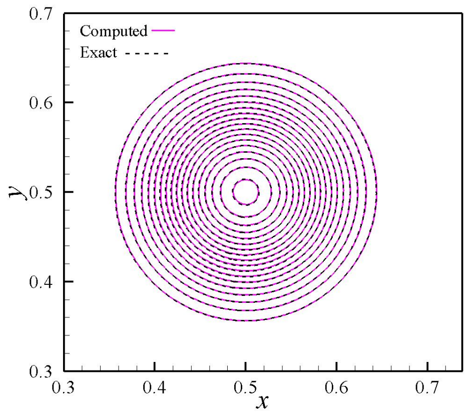

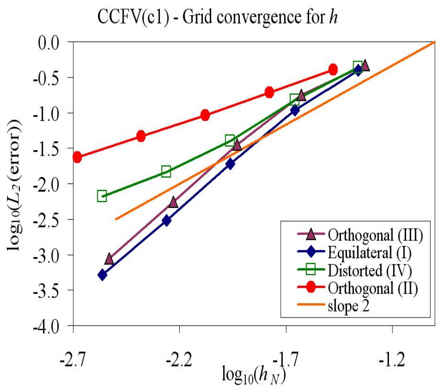
CCFV(c1) - Grid convergence for h
log10(L2(error))
log10(hN)
Orthogonal (III)
Equilateral (I)
Distorted (IV)
Orthogonal (II)
slope 2

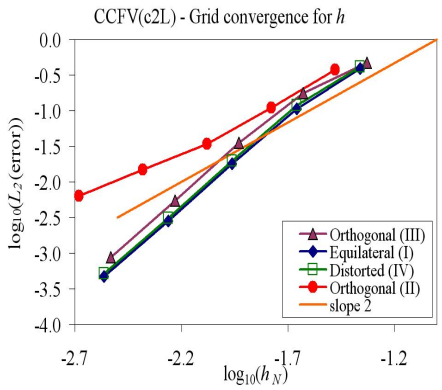
CCFV(c2L) - Grid convergence for h
log10(L2(error))
log10(hN)
Orthogonal (III)
Equilateral (I)
Distorted (IV)
Orthogonal (II)
slope 2

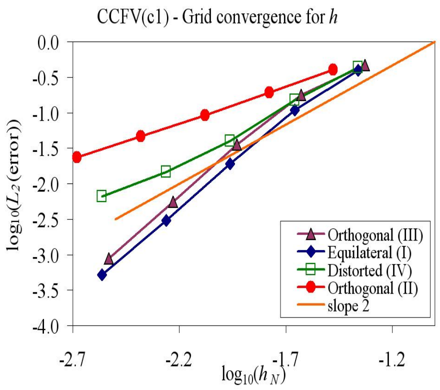
CCFV(c1) - Grid convergence for h
$\log_{10}(L_2(\text{error}))$
$\log_{10}(h_N)$
Orthogonal (III)
Equilateral (I)
Distorted (IV)
Orthogonal (II)
slope 2

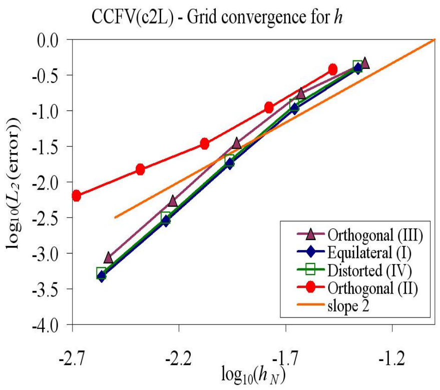
CCFV(c2L) - Grid convergence for h
$\log_{10}(L_2(\text{error}))$
$\log_{10}(h_N)$
Orthogonal (III)
Equilateral (I)
Distorted (IV)
Orthogonal (II)
slope 2

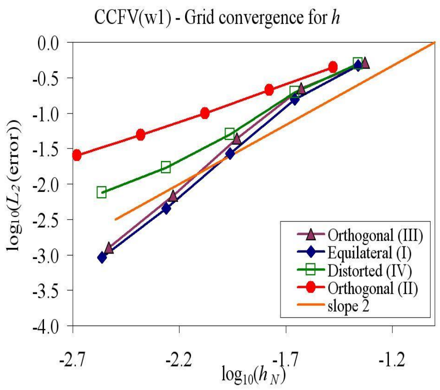
CCFV(w1) - Grid convergence for h
$\log_{10}(L_2(\text{error}))$
$\log_{10}(h_N)$
Orthogonal (III)
Equilateral (I)
Distorted (IV)
Orthogonal (II)
slope 2

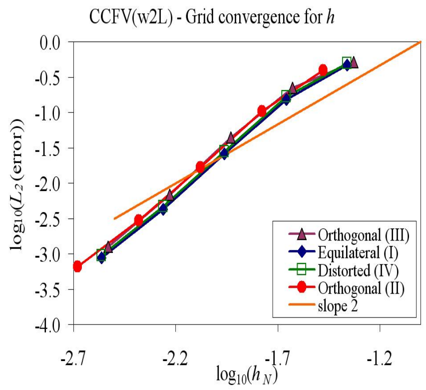
CCFV(w2L) - Grid convergence for h
$\log_{10}(L_2(\text{error}))$
$\log_{10}(h_N)$
Orthogonal (III)
Equilateral (I)
Distorted (IV)
Orthogonal (II)
slope 2

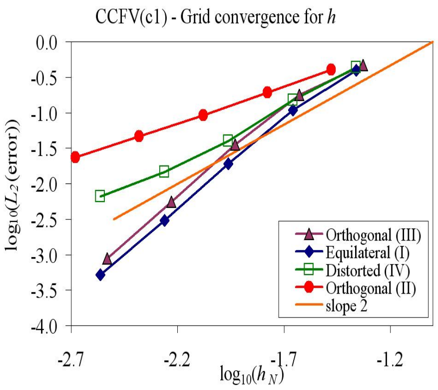
CCFV(c1) - Grid convergence for h
log10(L2(error))
log10(h_N)
Orthogonal (III)
Equilateral (I)
Distorted (IV)
Orthogonal (II)
slope 2

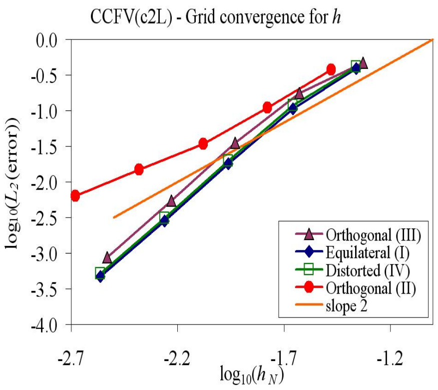
CCFV(c2L) - Grid convergence for h
log10(L2(error))
log10(h_N)
Orthogonal (III)
Equilateral (I)
Distorted (IV)
Orthogonal (II)
slope 2

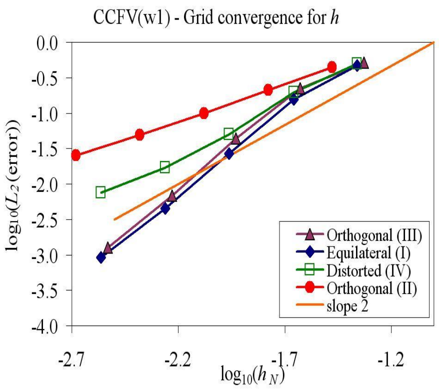
CCFV(w1) - Grid convergence for h
log10(L2(error))
log10(h_N)
Orthogonal (III)
Equilateral (I)
Distorted (IV)
Orthogonal (II)
slope 2

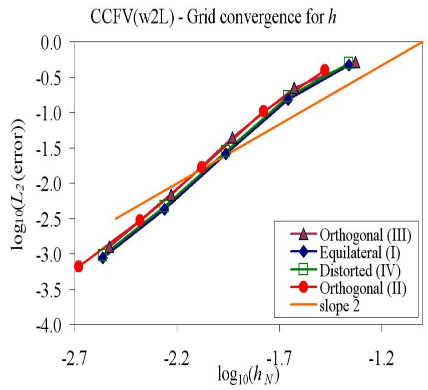
CCFV(w2L) - Grid convergence for h
log10(L2(error))
log10(h_N)
Orthogonal (III)
Equilateral (I)
Distorted (IV)
Orthogonal (II)
slope 2

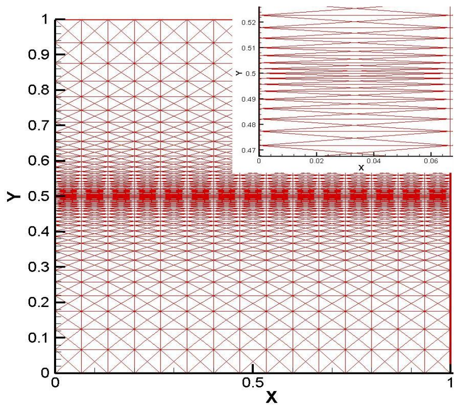
Y
X

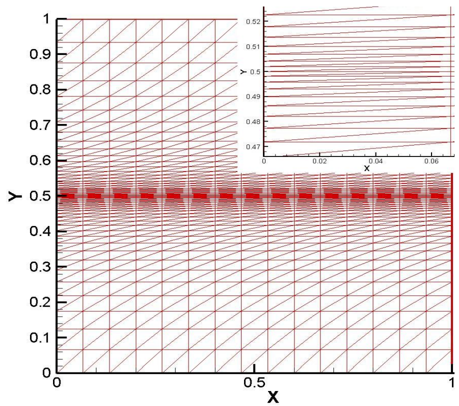
Y
X

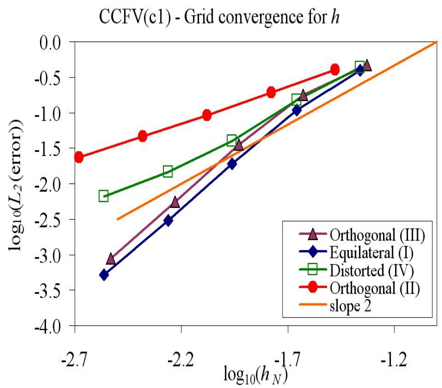
CCFV(c1) - Grid convergence for h
log10(L2(error))
log10(hN)
Orthogonal (III)
Equilateral (I)
Distorted (IV)
Orthogonal (II)
slope 2

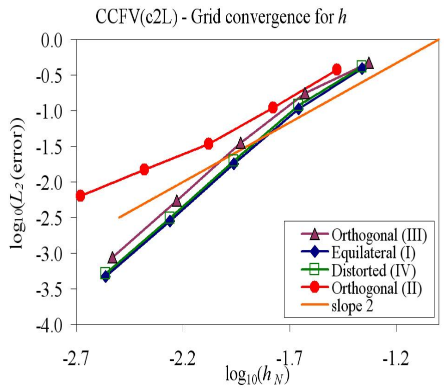
CCFV(c2L) - Grid convergence for h
log10(L2(error))
log10(hN)
Orthogonal (III)
Equilateral (I)
Distorted (IV)
Orthogonal (II)
slope 2

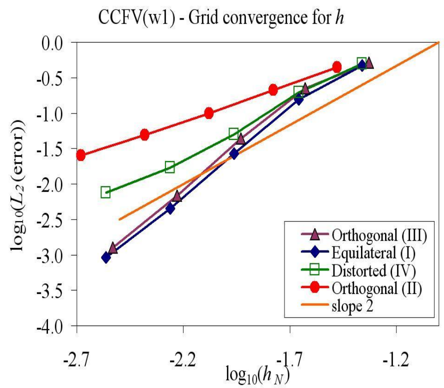
CCFV(w1) - Grid convergence for h
log10(L2(error))
log10(hN)
Orthogonal (III)
Equilateral (I)
Distorted (IV)
Orthogonal (II)
slope 2

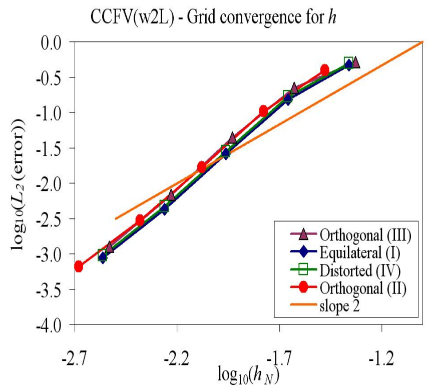
CCFV(w2L) - Grid convergence for h
log10(L2(error))
log10(hN)
Orthogonal (III)
Equilateral (I)
Distorted (IV)
Orthogonal (II)
slope 2

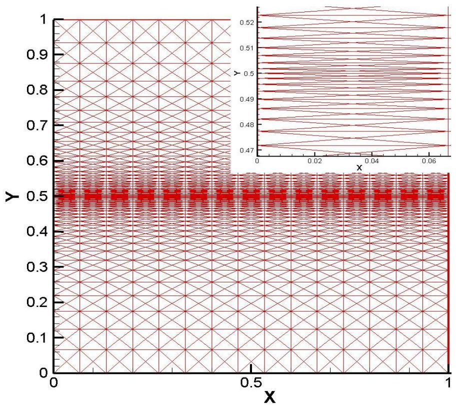
Y
X

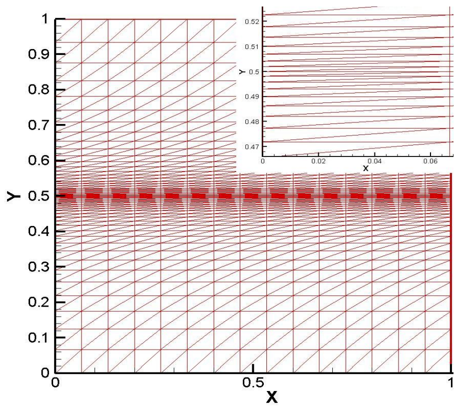
Y
X

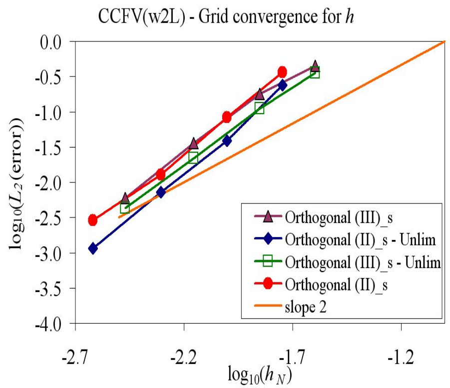
CCFV(w2L) - Grid convergence for h
log10(L2(error))
log10(hN)
Orthogonal (III)_s
Orthogonal (II)_s - Unlim
Orthogonal (III)_s - Unlim
Orthogonal (II)_s
slope 2

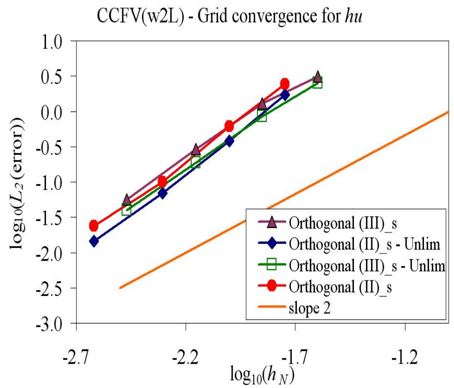
CCFV(w2L) - Grid convergence for hu
log10(L2(error))
log10(hN)
Orthogonal (III)_s
Orthogonal (II)_s - Unlim
Orthogonal (III)_s - Unlim
Orthogonal (II)_s
slope 2

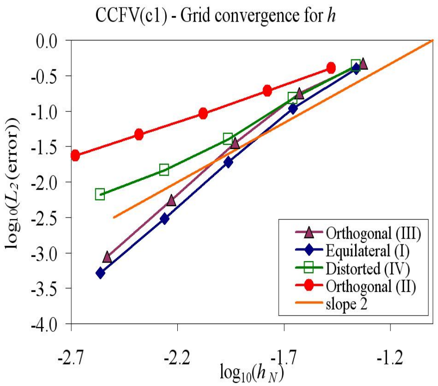
CCFV(c1) - Grid convergence for h
log10(L2(error))
log10(hN)
Orthogonal (III)
Equilateral (I)
Distorted (IV)
Orthogonal (II)
slope 2

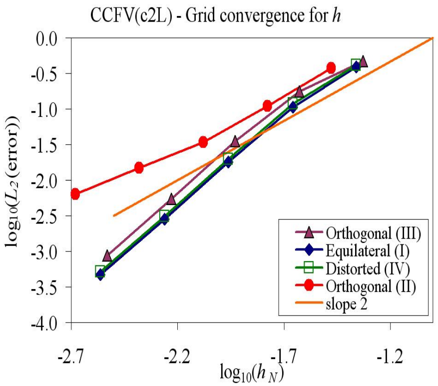
CCFV(c2L) - Grid convergence for h
log10(L2(error))
log10(hN)
Orthogonal (III)
Equilateral (I)
Distorted (IV)
Orthogonal (II)
slope 2

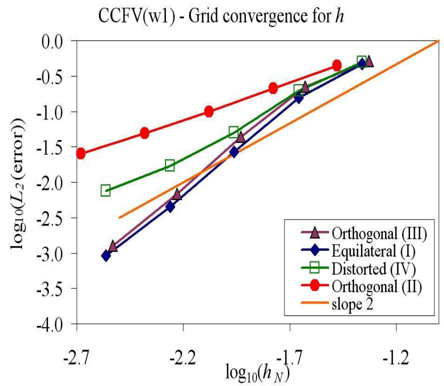
CCFV(w1) - Grid convergence for h
log10(L2(error))
log10(hN)
Orthogonal (III)
Equilateral (I)
Distorted (IV)
Orthogonal (II)
slope 2

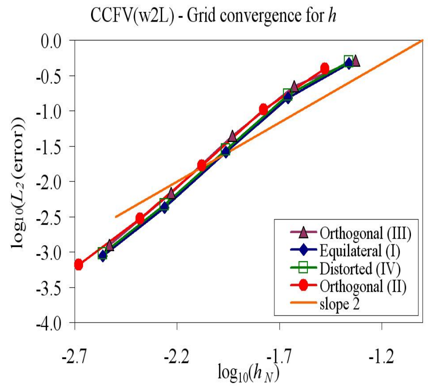
CCFV(w2L) - Grid convergence for h
log10(L2(error))
log10(hN)
Orthogonal (III)
Equilateral (I)
Distorted (IV)
Orthogonal (II)
slope 2

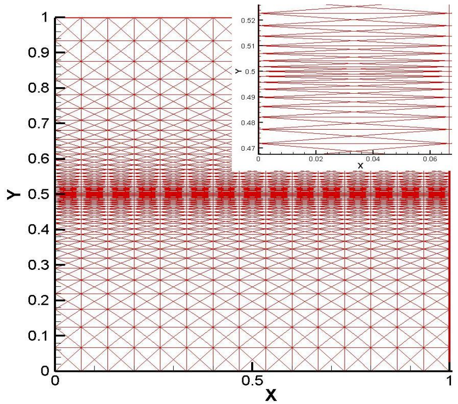
Y
X

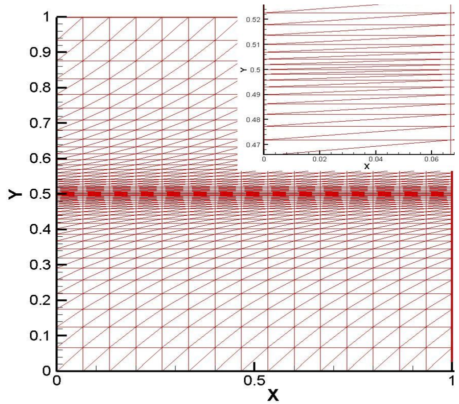
Y
X

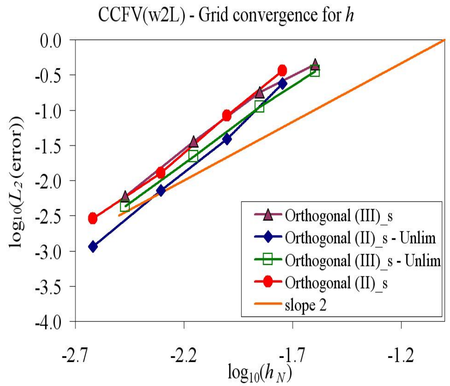
CCFV(w2L) - Grid convergence for h
log10(L2(error))
log10(hN)
Orthogonal (III)_s
Orthogonal (II)_s - Unlim
Orthogonal (III)_s - Unlim
Orthogonal (II)_s
slope 2

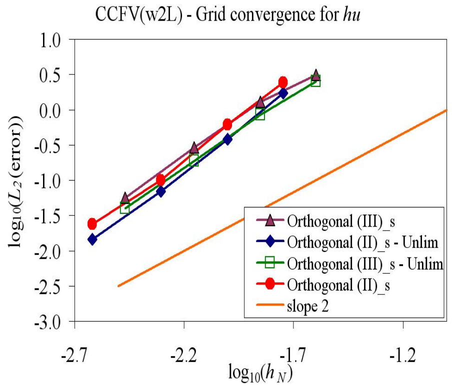
CCFV(w2L) - Grid convergence for hu
log10(L2(error))
log10(hN)
Orthogonal (III)_s
Orthogonal (II)_s - Unlim
Orthogonal (III)_s - Unlim
Orthogonal (II)_s
slope 2

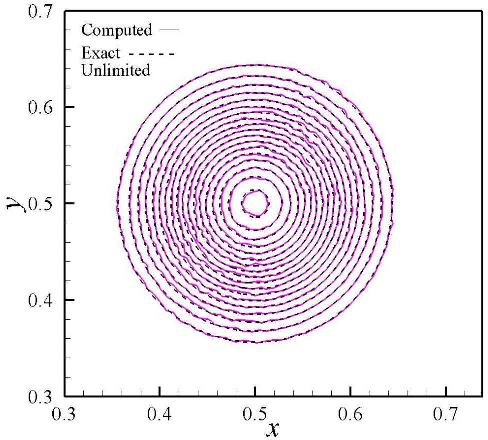
Computed
Exact
Unlimited
y
x

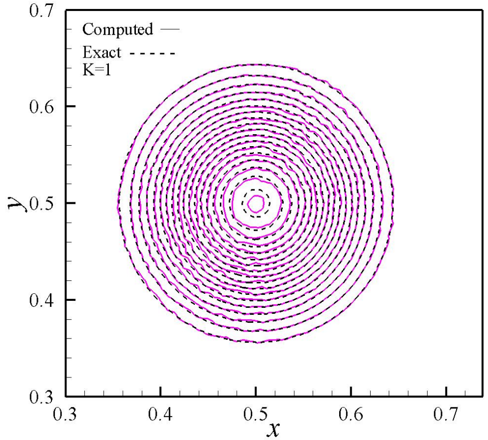
Computed
Exact
K=1
y
x

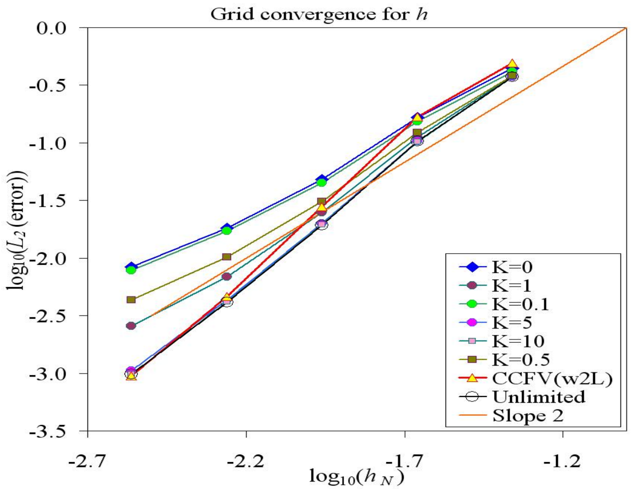
Grid convergence for h
log10(L2(error))
log10(hN)
K=0
K=1
K=0.1
K=5
K=10
K=0.5
CCFV(w2L)
Unlimited
Slope 2

Ib A 2D potential (steady) solution with topography

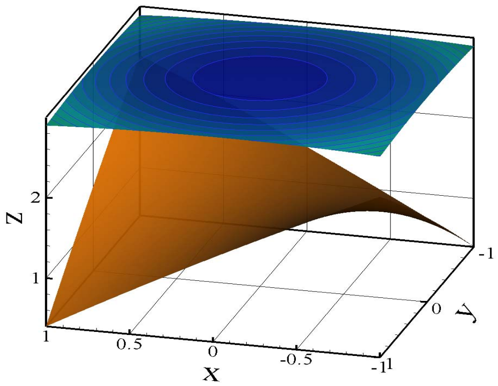

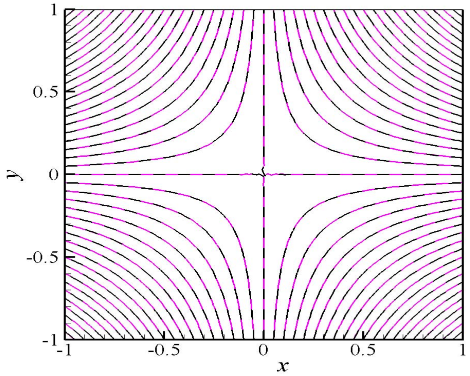

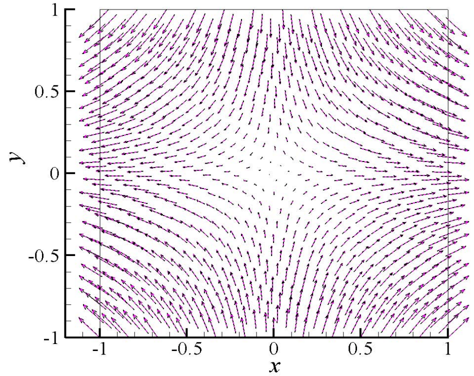

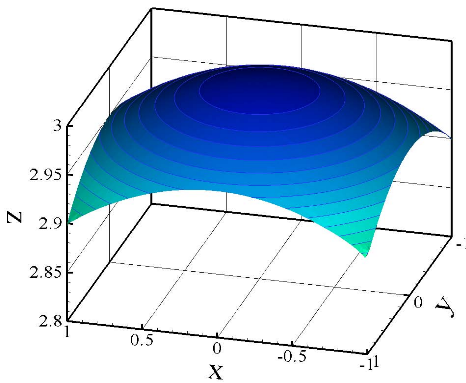

Ib A 2D potential (steady) solution with topography

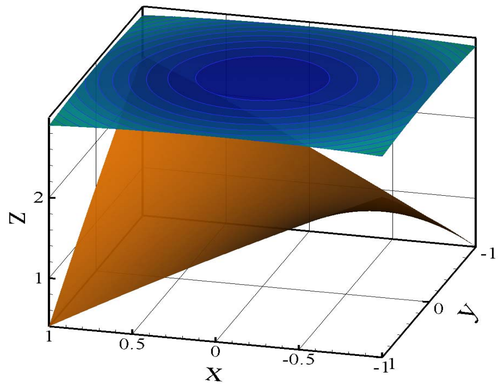

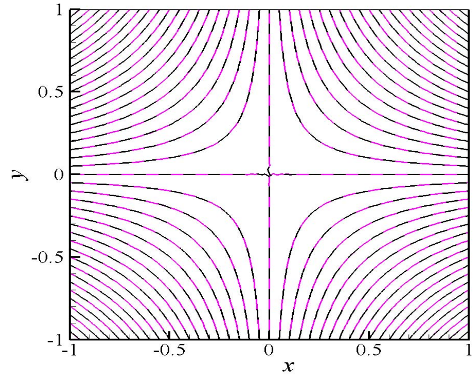

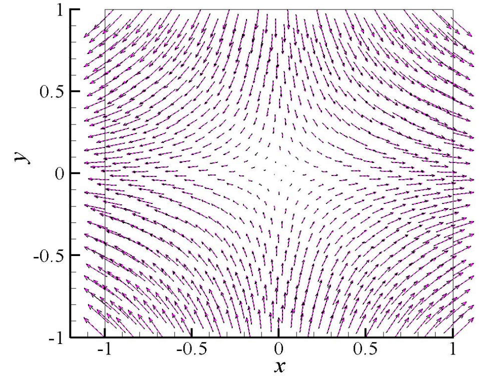

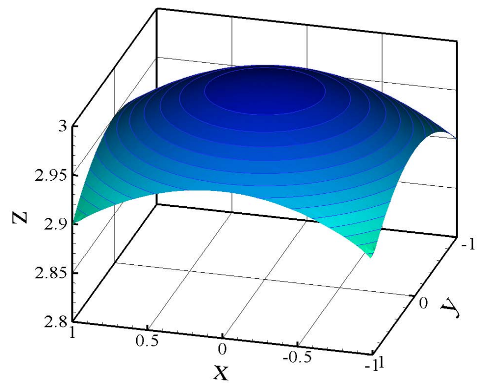

Unlimited - Orthogonal (II)

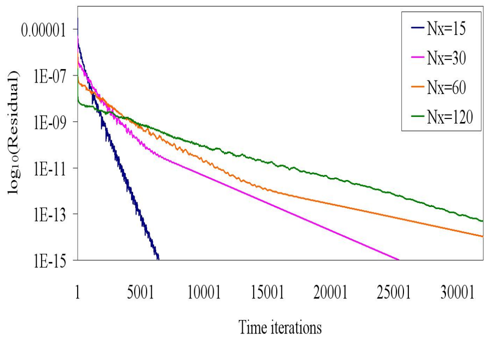

K=1 - Orthogonal (II)

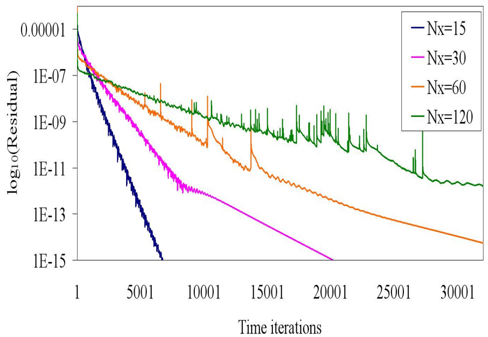

CCFV(c2L) - Orthogonal (II)

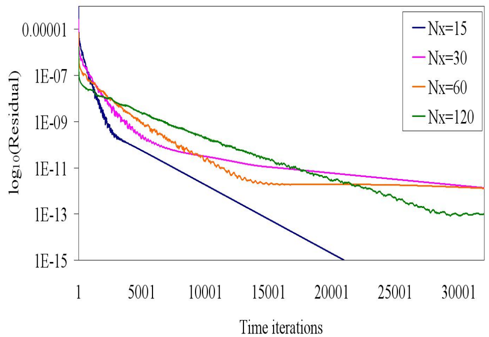

CCFV(w2L) - Orthogonal (II)

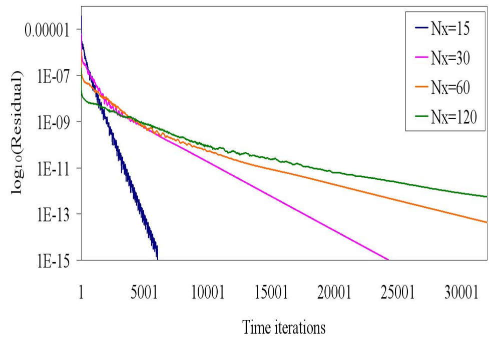

Ib A 2D potential (steady) solution with topography

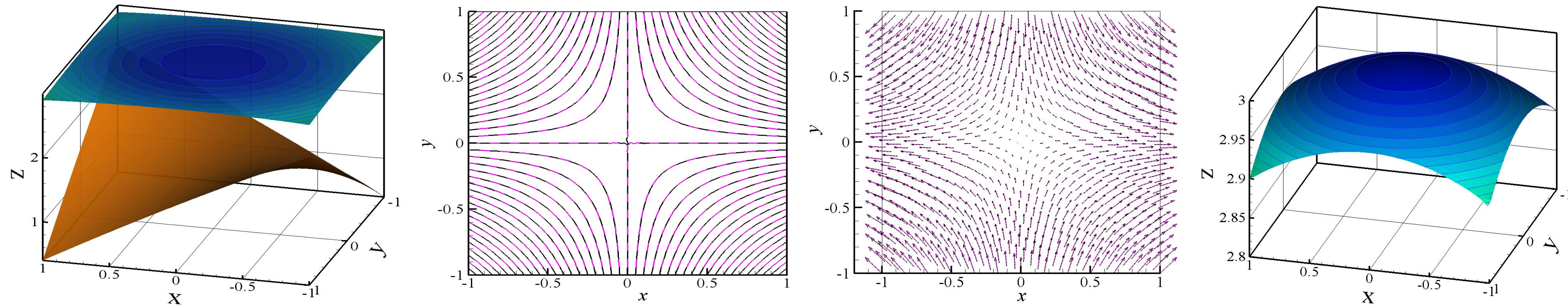

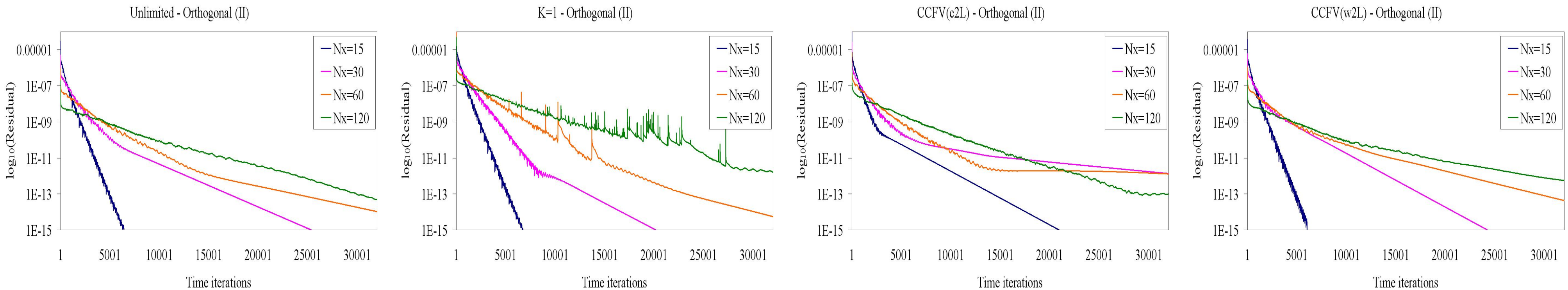

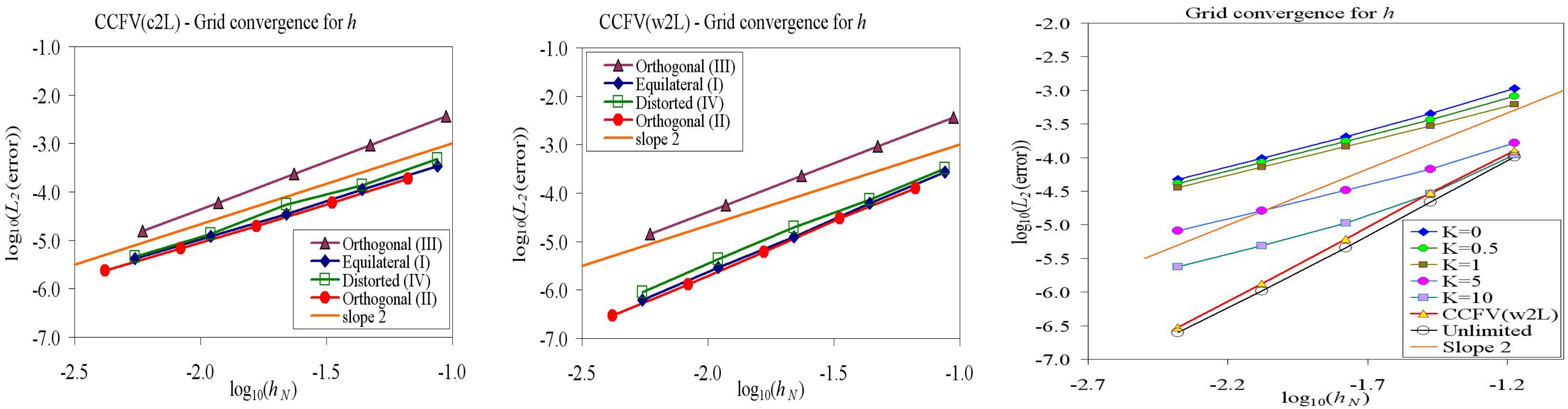

Ic A 2D Riemann problem

$$\Omega = [-100, 100] \times [-100, 100],\, N = 4000$$

Ic A 2D Riemann problem

$$\Omega = [-100, 100] \times [-100, 100], N = 4000$$

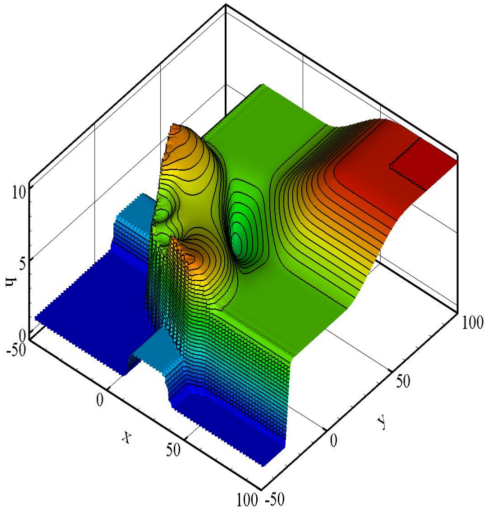

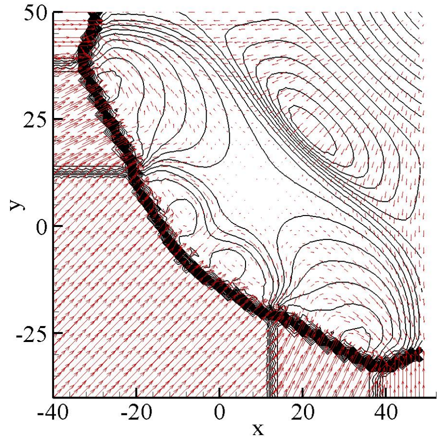

(h) 1st order scheme on a type-II grid

Ic A 2D Riemann problem

$$\Omega = [-100, 100] \times [-100, 100], N = 4000$$

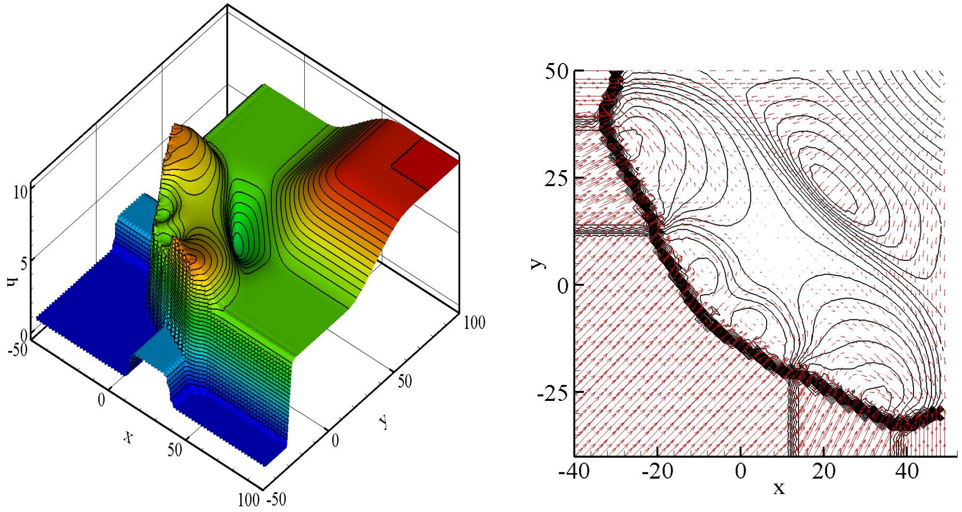

(h) 1st order scheme on a type-II grid

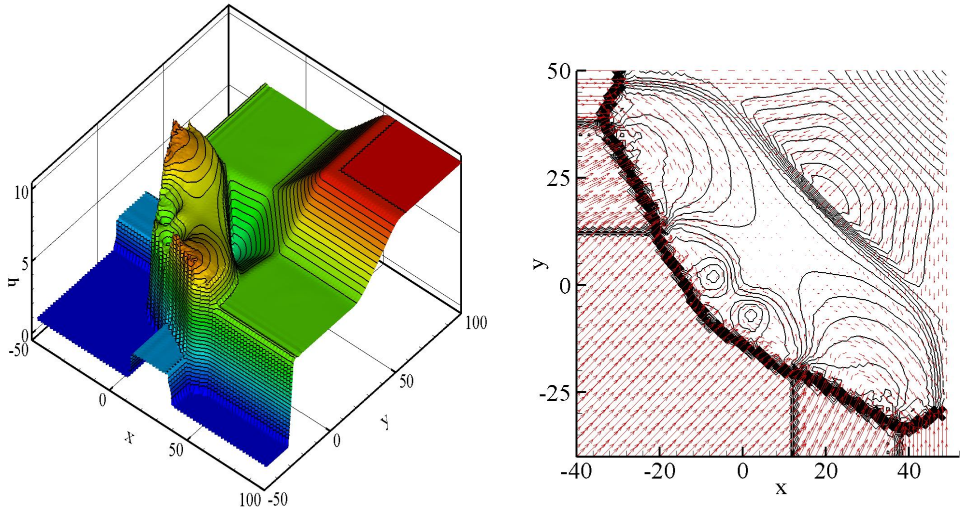

(i) CCFVw2L scheme on a type-II grid

Ic A 2D Riemann problem

$$\Omega = [-100, 100] \times [-100, 100], N = 4000$$

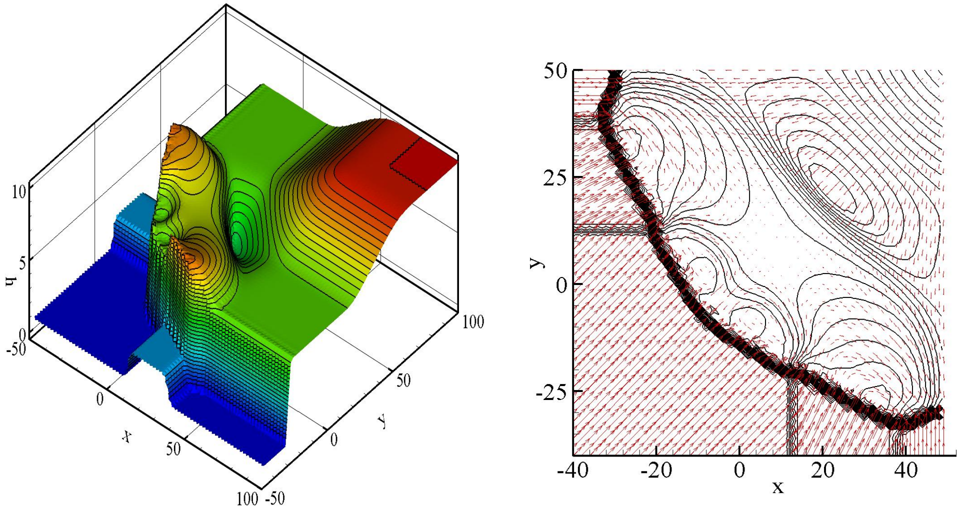

(h) 1st order scheme on a type-II grid

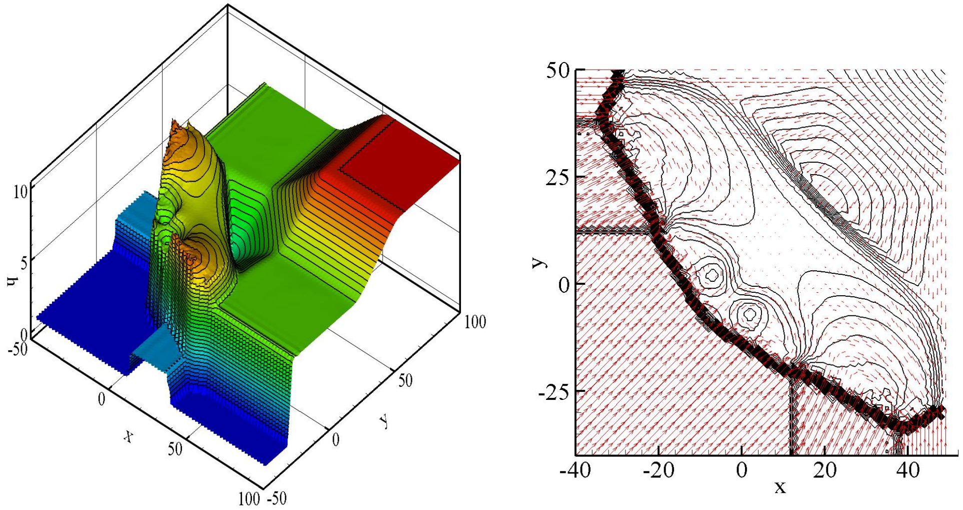

(i) CCFVw2L scheme on a type-II grid

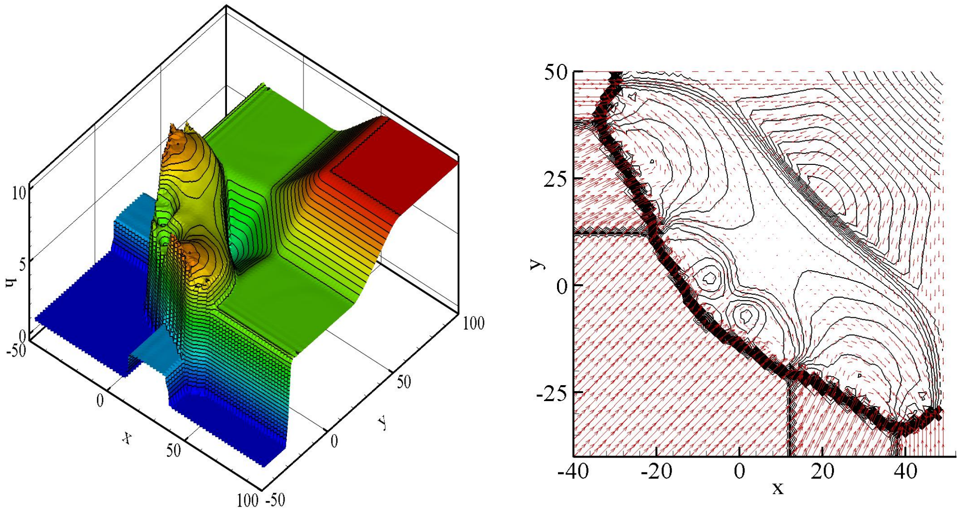

(j) V-scheme ($K = 0$) on a type-II grid

Ic A 2D Riemann problem

$$\Omega = [-100, 100] \times [-100, 100], N = 4000$$

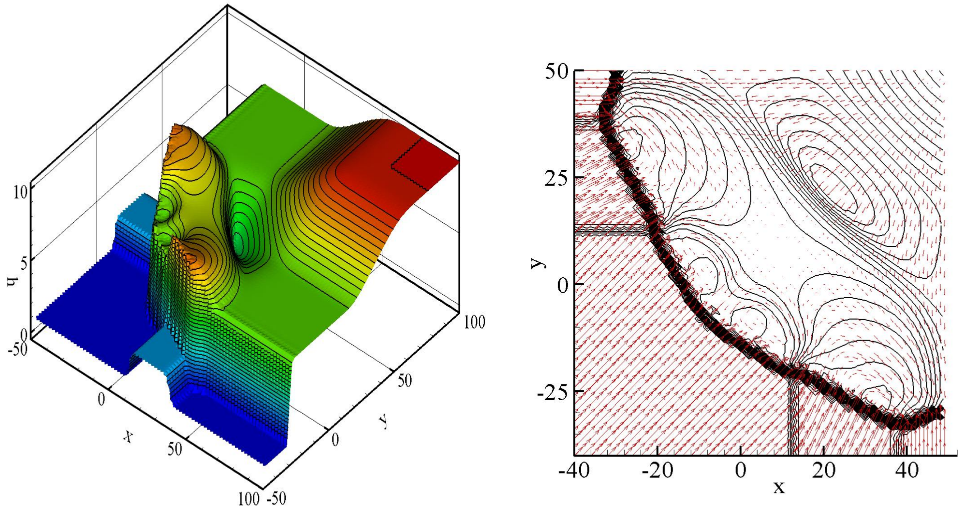

(h) 1st order scheme on a type-II grid

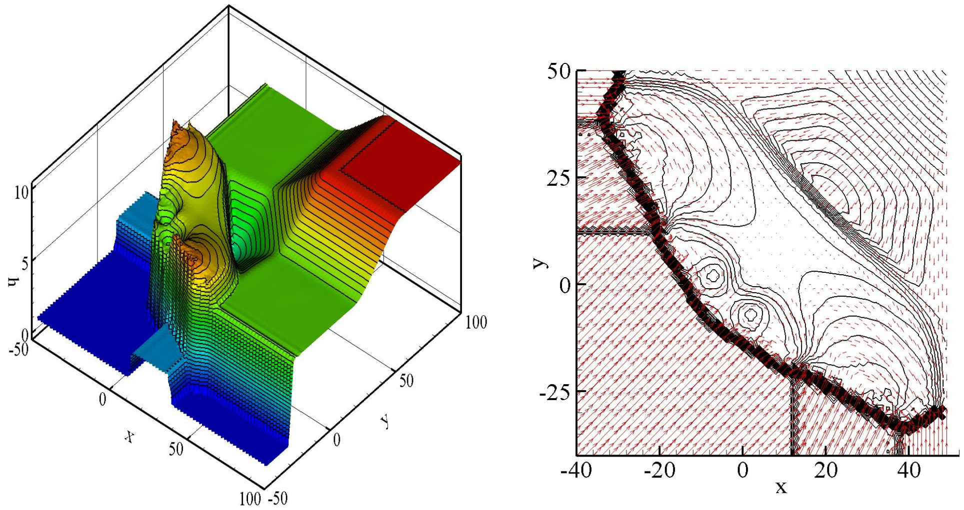

(i) CCFVw2L scheme on a type-II grid

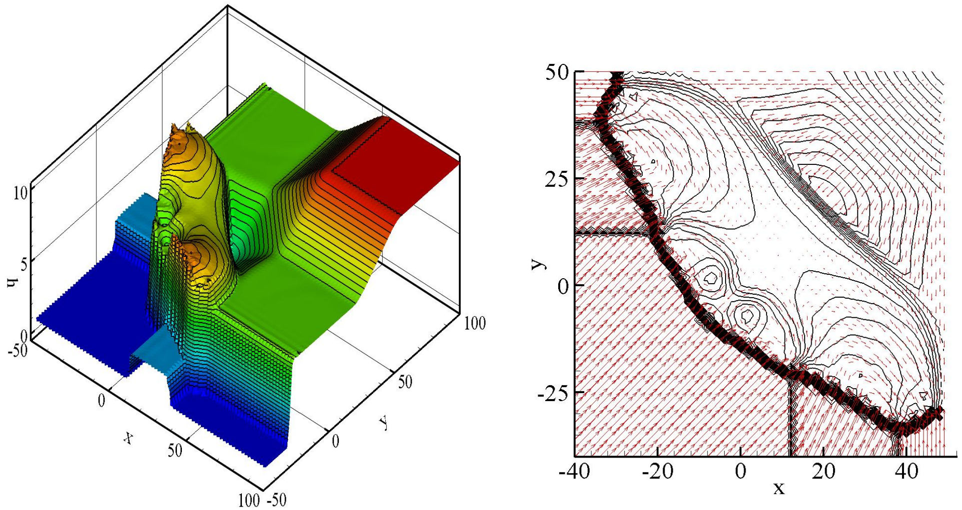

(j) V-scheme ($K = 0$) on a type-II grid

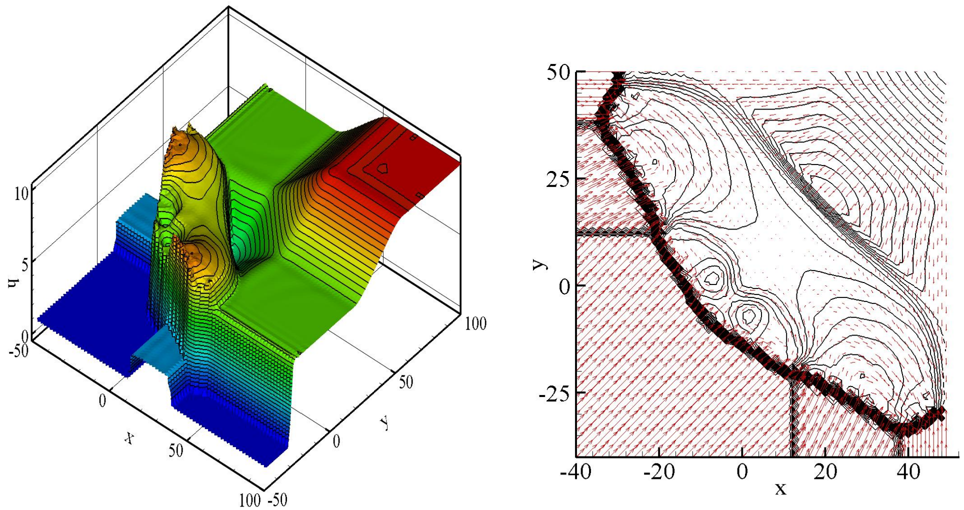

(k) V-scheme ($K = 1$) on a type-II grid

Numerical results and Comparisons II (Euler equations)

IIa A traveling vortex solution

HLLC solver used for all schemes

Numerical results and Comparisons II (Euler equations)

IIa A traveling vortex solution

HLLC solver used for all schemes

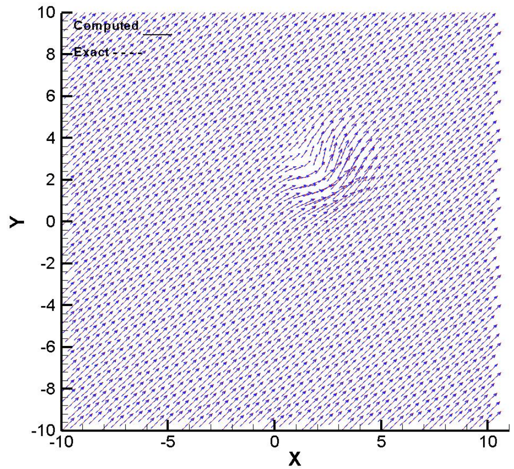

Numerical results and Comparisons II (Euler equations)

IIa A traveling vortex solution

HLLC solver used for all schemes

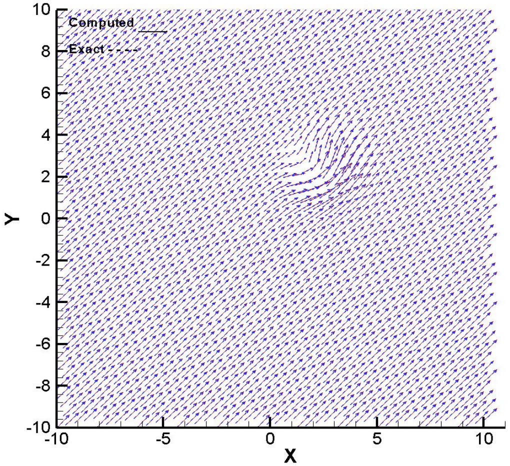

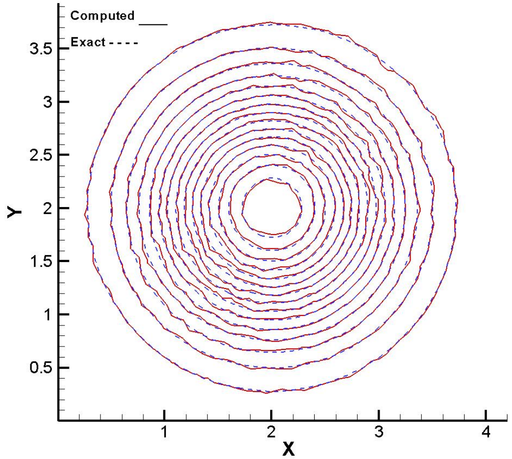

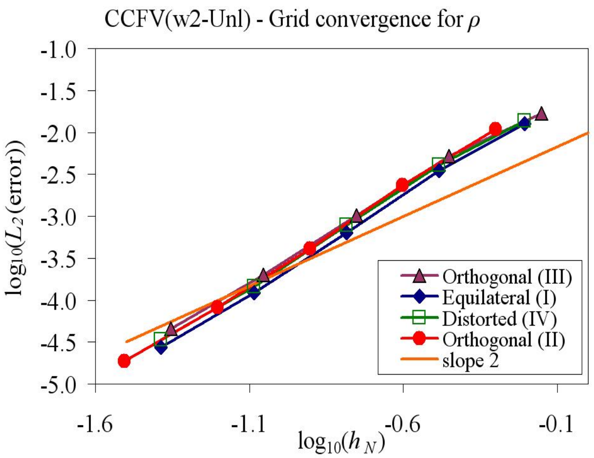

Numerical results and Comparisons II (Euler equations)

IIa A traveling vortex solution

HLLC solver used for all schemes

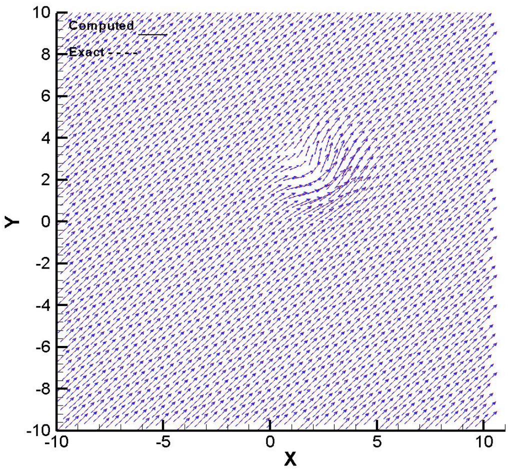

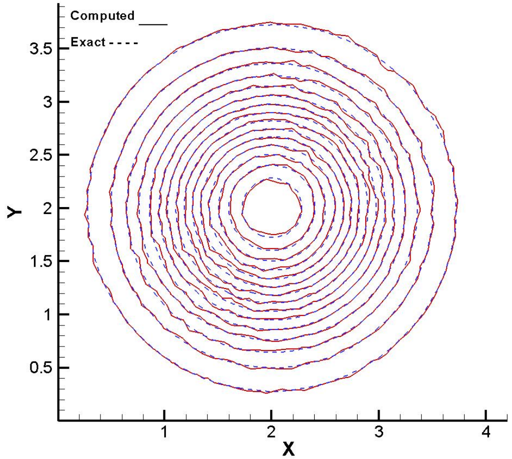

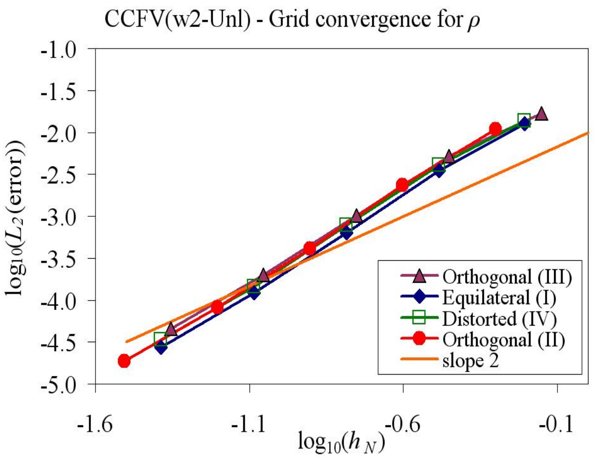

Numerical results and Comparisons II (Euler equations)

IIa A traveling vortex solution

HLLC solver used for all schemes

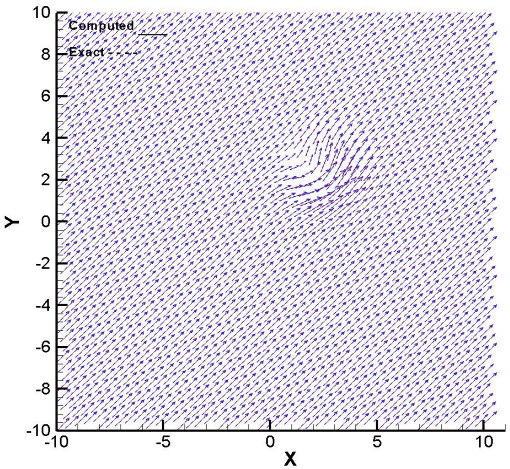

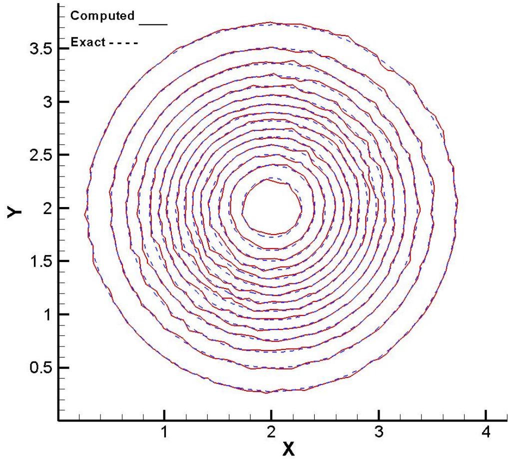

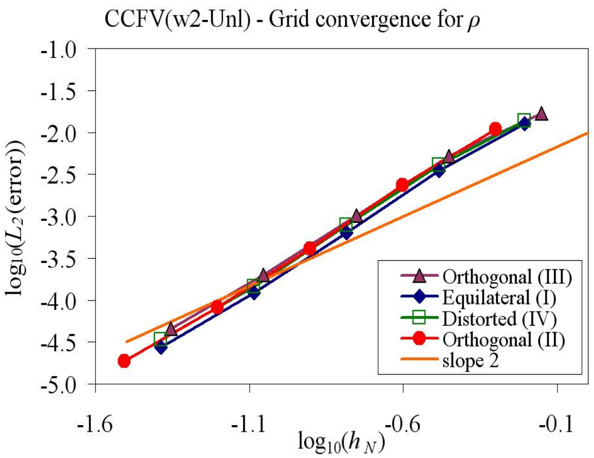

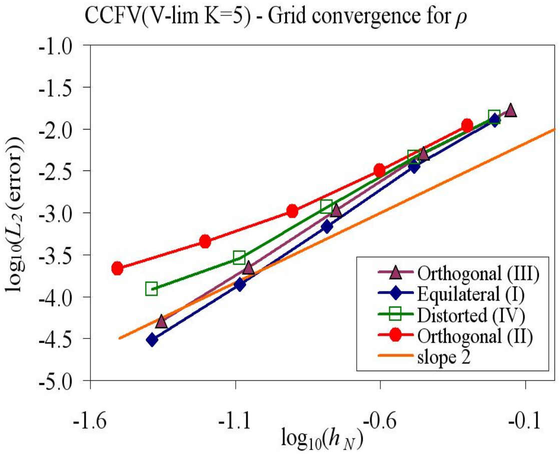

Numerical results and Comparisons II (Euler equations)

IIa A traveling vortex solution

HLLC solver used for all schemes

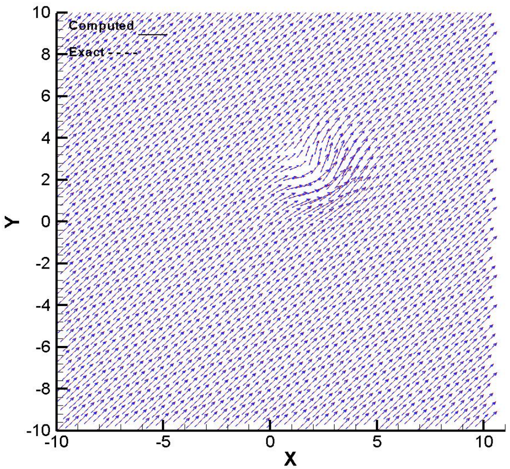

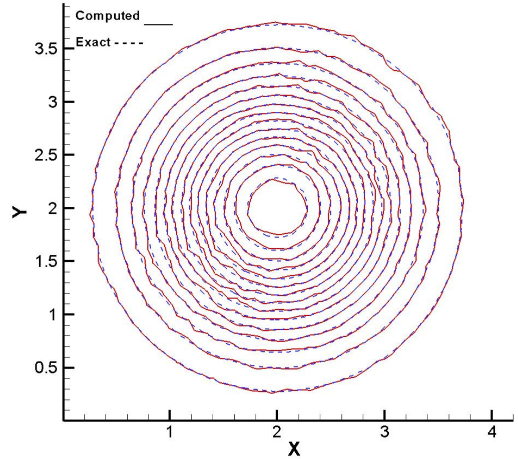

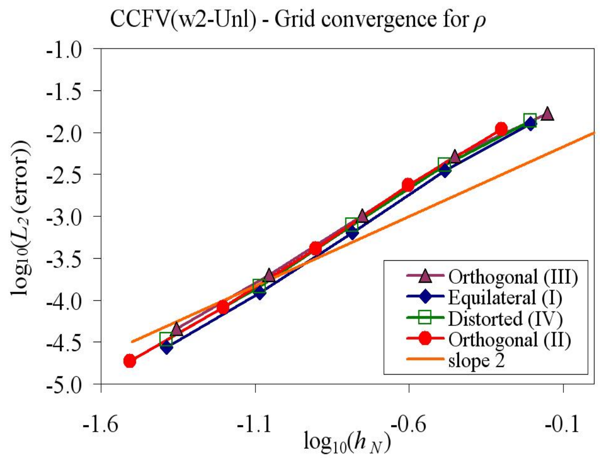

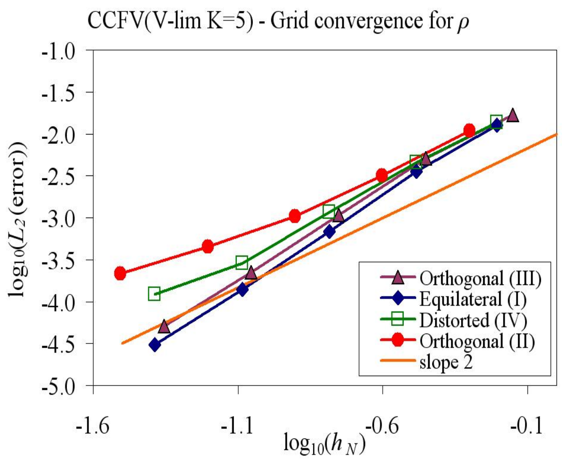

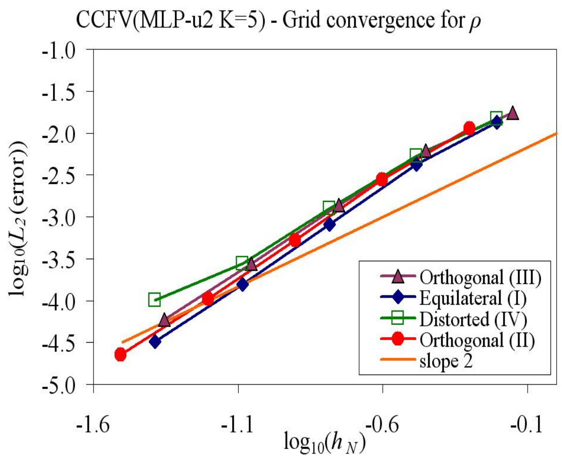

Numerical results and Comparisons II (Euler equations)

IIa A traveling vortex solution

HLLC solver used for all schemes

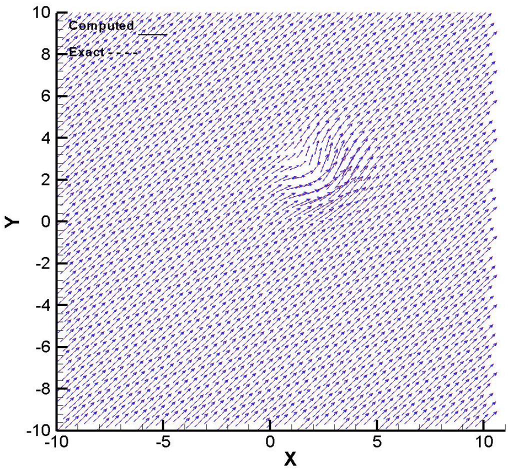

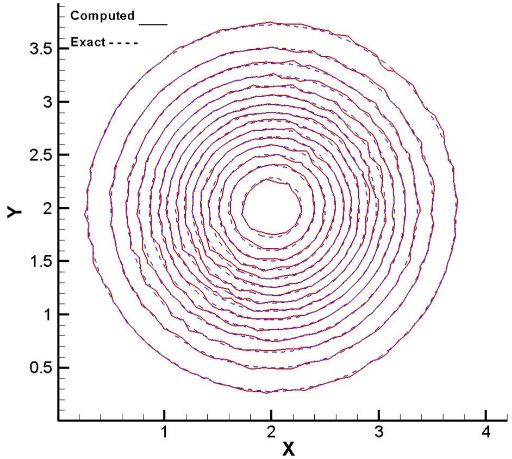

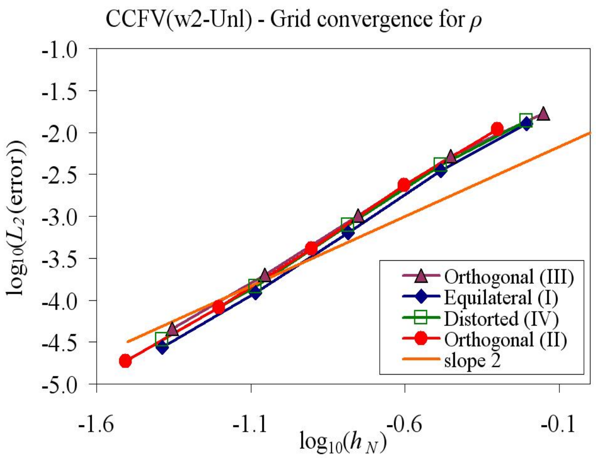

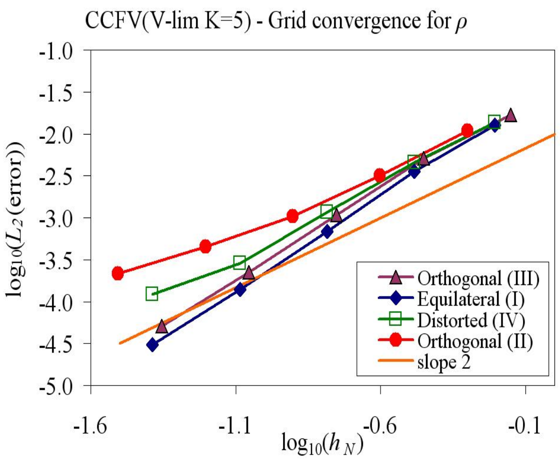

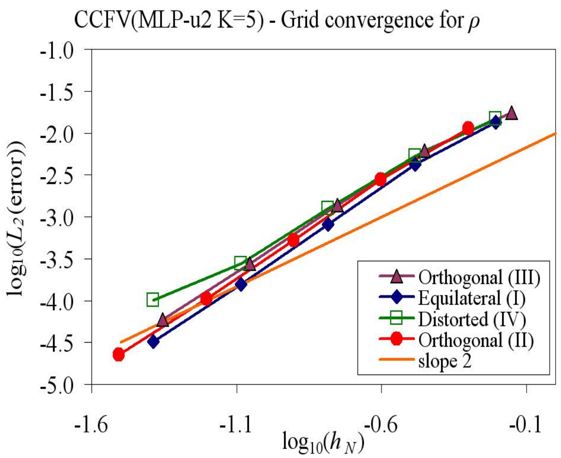

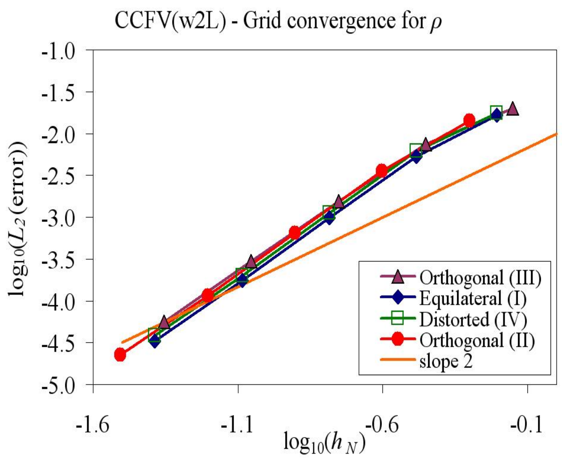

IIa A traveling vortex solution at $t = 2T$ (On a type-IV distorted mesh)

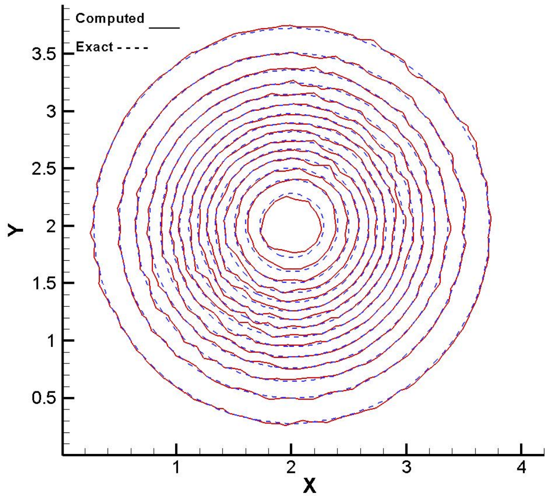

(l) V-scheme $(K = 1)$

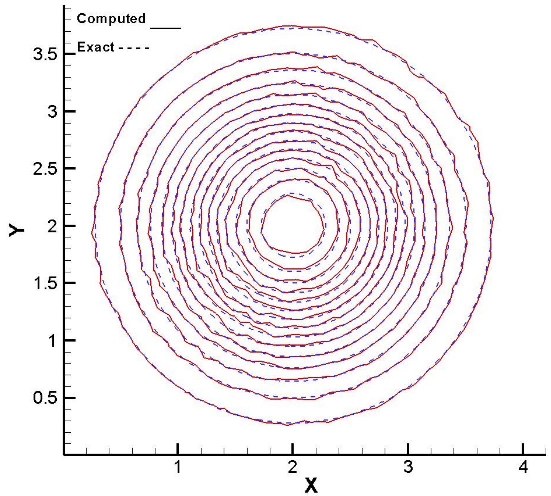

(m) MLPu2 $(K = 1)$

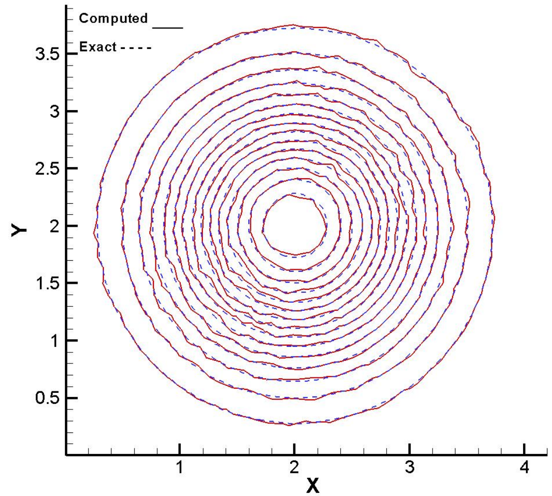

(n) CCVFw2L scheme

IIb Some classical test problems

HLLC solver, $N = 16000$ on a type-II mesh, CFL= 0.5

$\texttt{IIb}$ Some classical test problems

HLLC solver, $N = 16000$ on a type-II mesh, CFL= 0.5

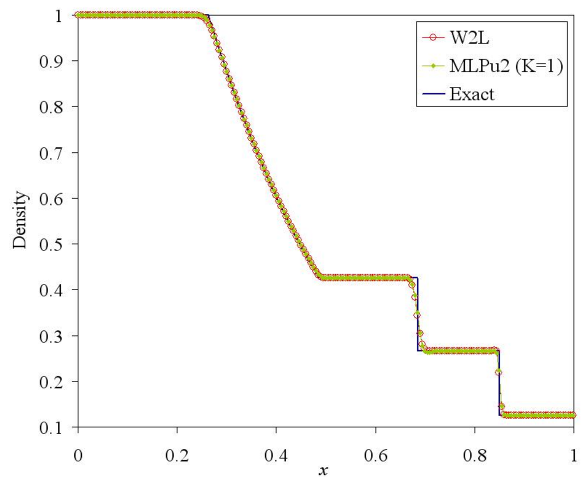

HLLC solver, $N = 16000$ on a type-II mesh, CFL= 0.5

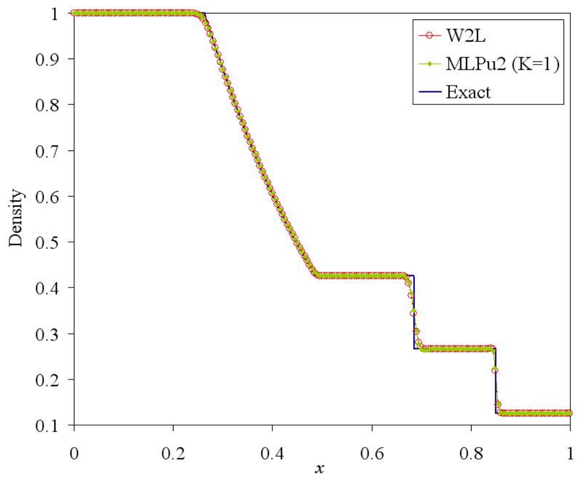

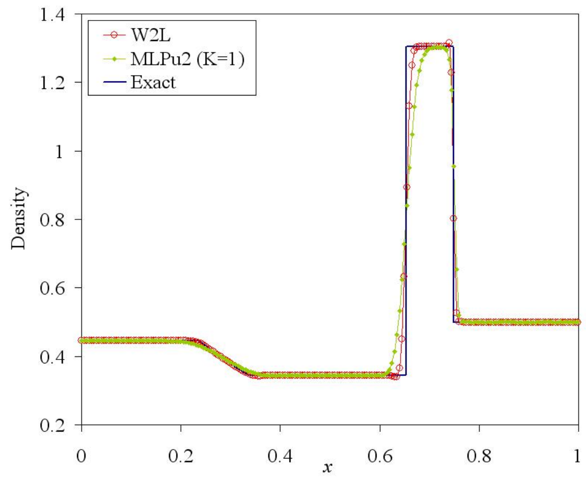

HLLC solver, $N = 16000$ on a type-II mesh, CFL= 0.5

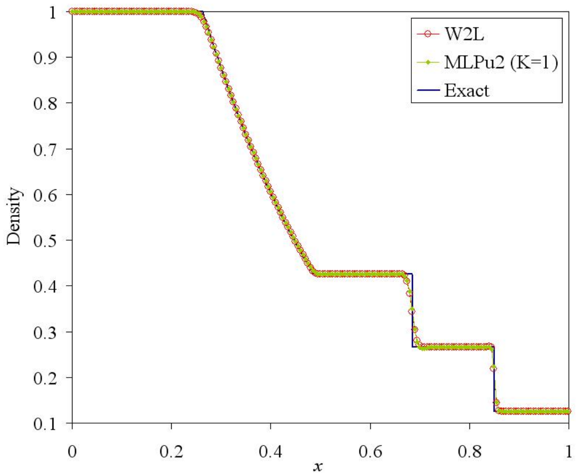

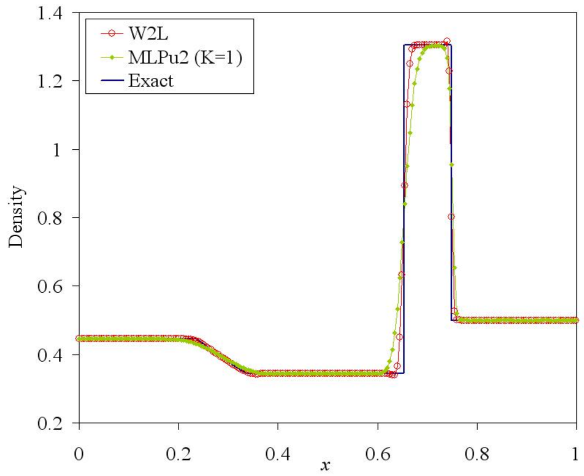

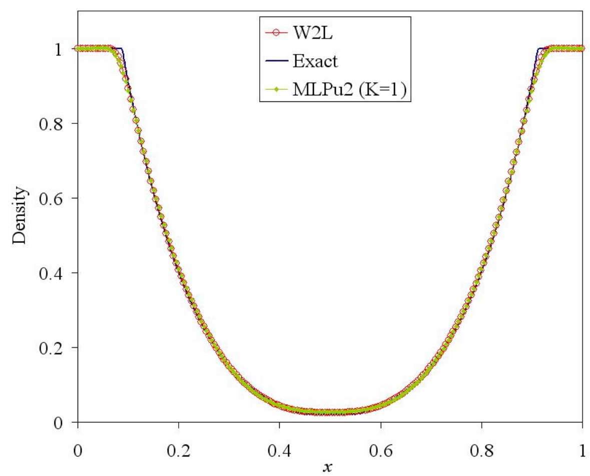

IIb Some classical test problems

HLLC solver, $N = 16000$ on a type-II mesh, CFL= 0.5

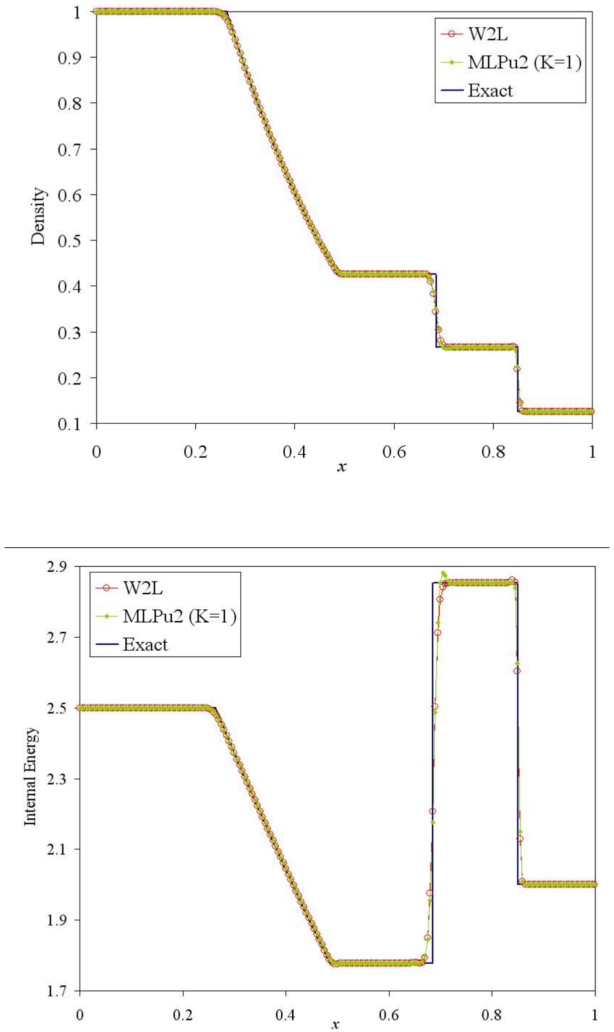

(o) **Sod's problem**

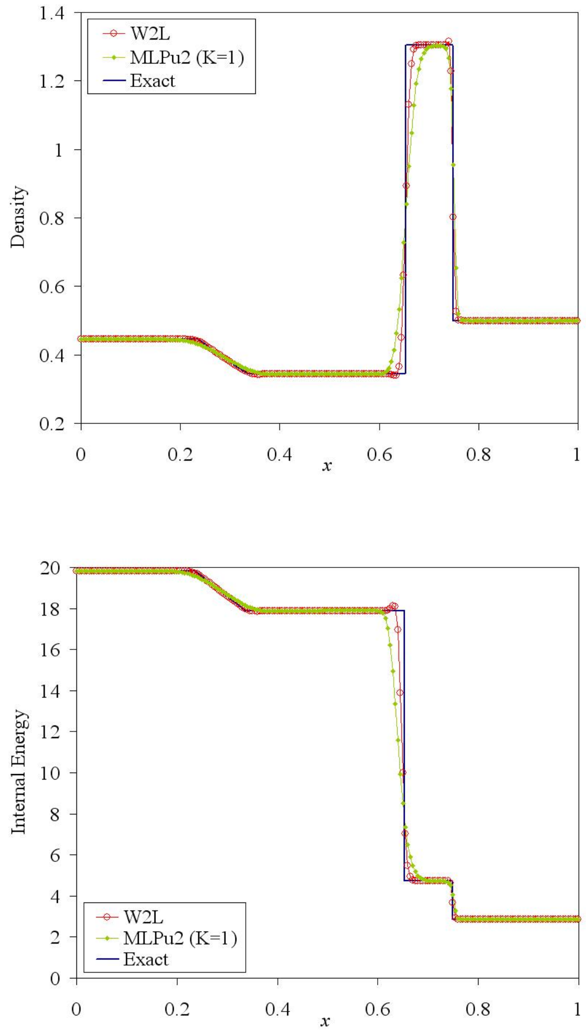

(p) **Harten-Lax problem**

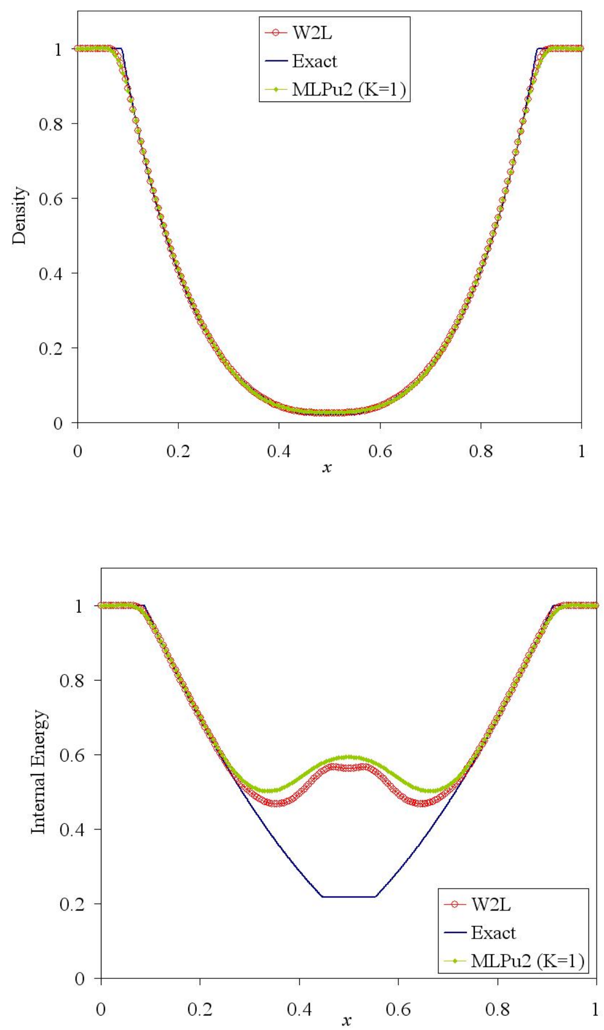

(q) **Supersonic expansion**

IIc Transonic flow around NACA 0012 airfoil

Case of M=0.8 and $\alpha = 1.25°$, HLLC solver, $N = 6492$ with 200 surface points

IIc Transonic flow around NACA 0012 airfoil

Case of M=0.8 and $\alpha = 1.25°$, HLLC solver, $N = 6492$ with 200 surface points

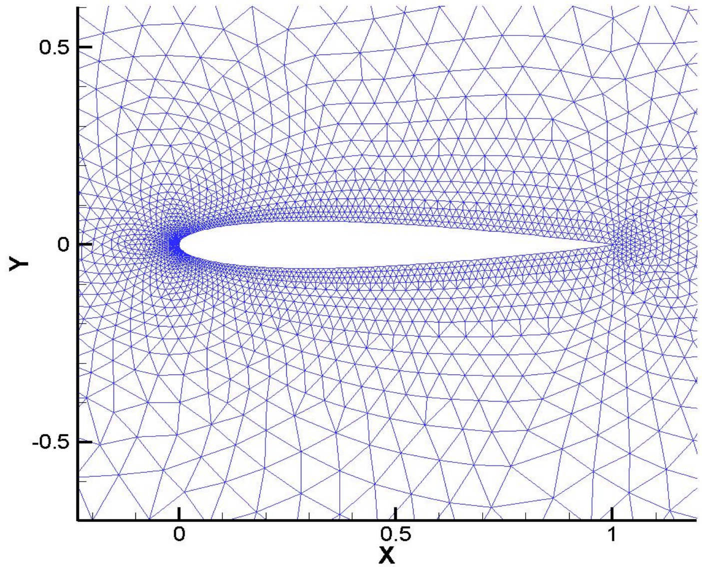

`IIc` Transonic flow around NACA 0012 airfoil

Case of M=0.8 and $\alpha = 1.25°$, HLLC solver, $N = 6492$ with 200 surface points

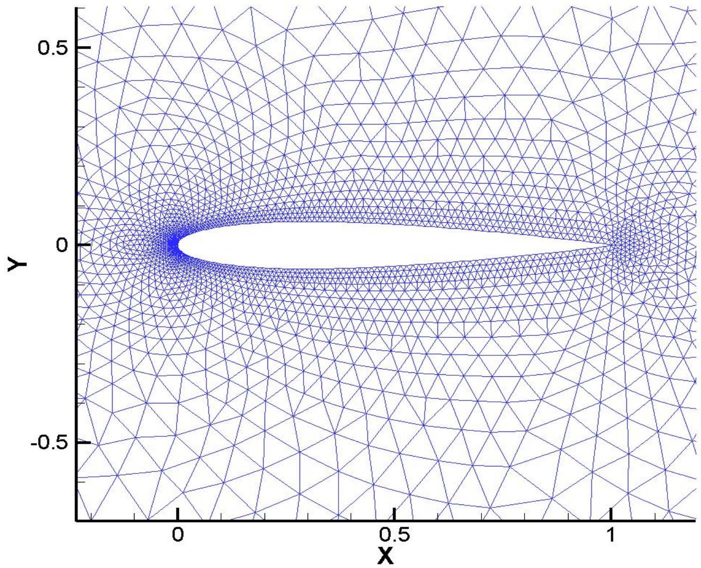

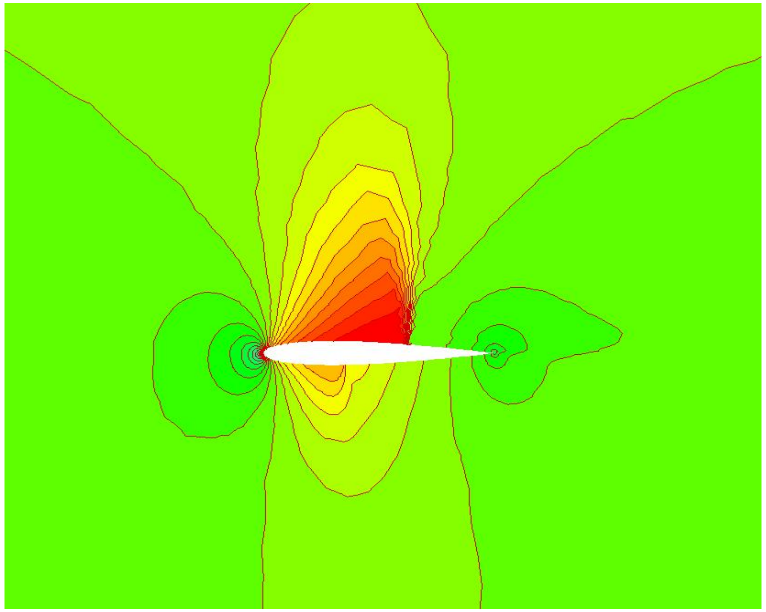

`IIc` Transonic flow around NACA 0012 airfoil

Case of M=0.8 and $\alpha = 1.25°$, HLLC solver, $N = 6492$ with 200 surface points

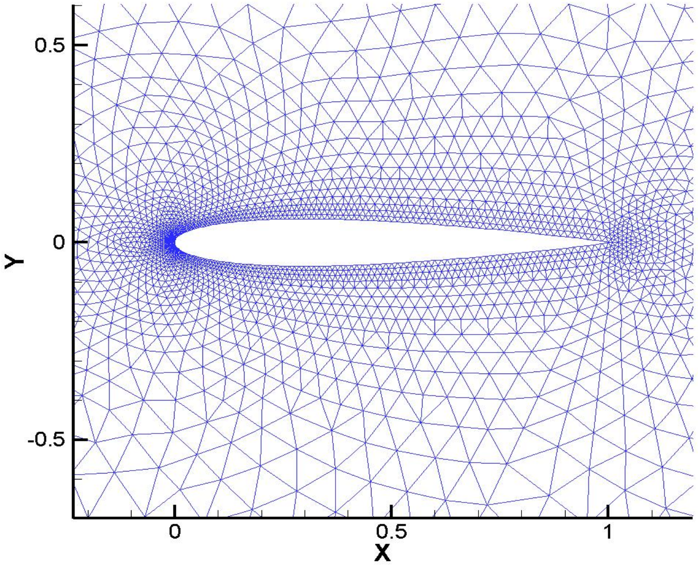

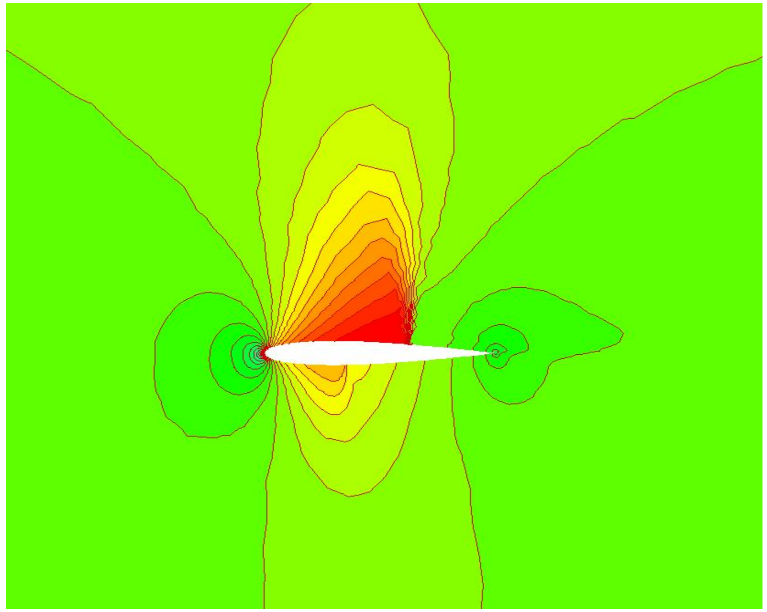

IIc Transonic flow around NACA 0012 airfoil

Case of M=0.8 and $\alpha = 1.25°$, HLLC solver, $N = 6492$ with 200 surface points

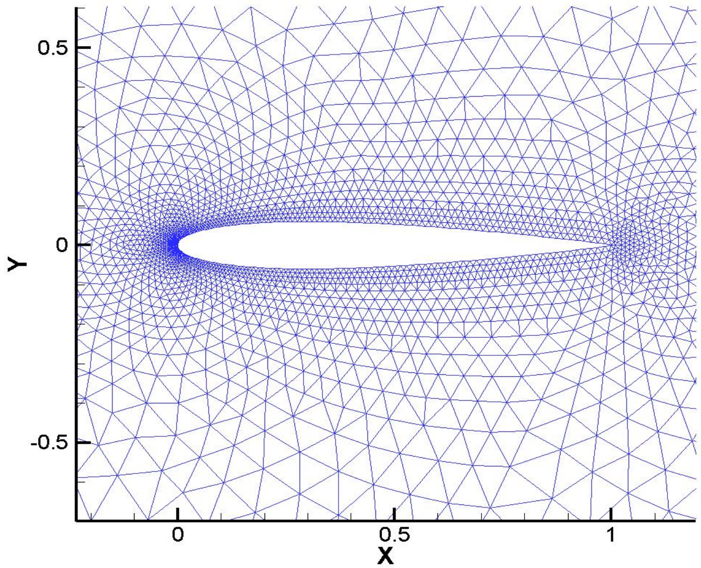

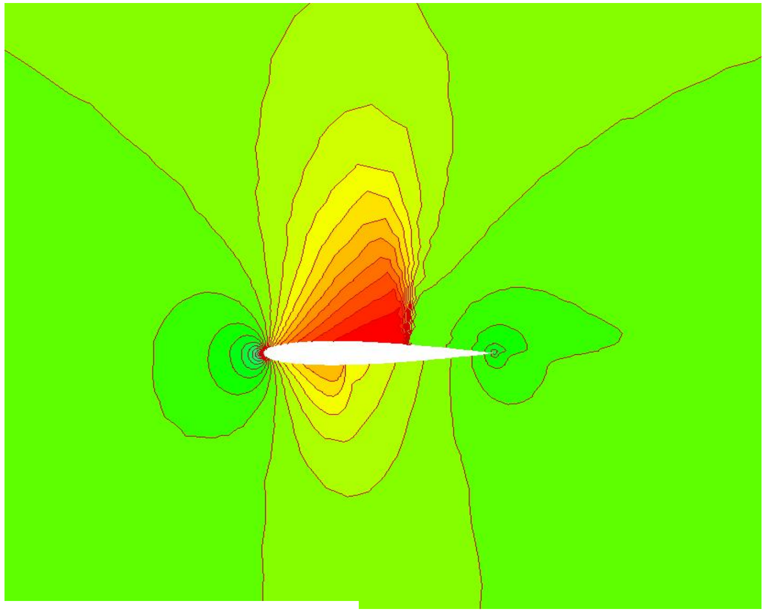

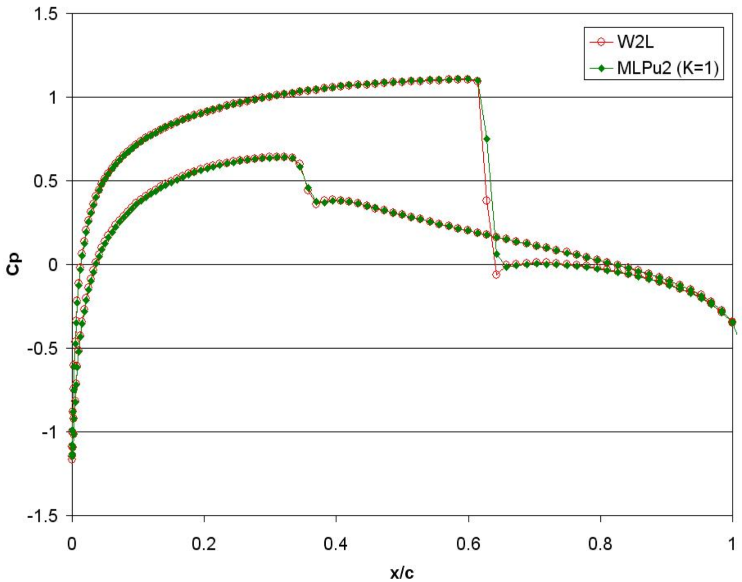

IIc Transonic flow around NACA 0012 airfoil

Case of M=0.8 and $\alpha = 1.25°$, HLLC solver, $N = 6492$ with 200 surface points

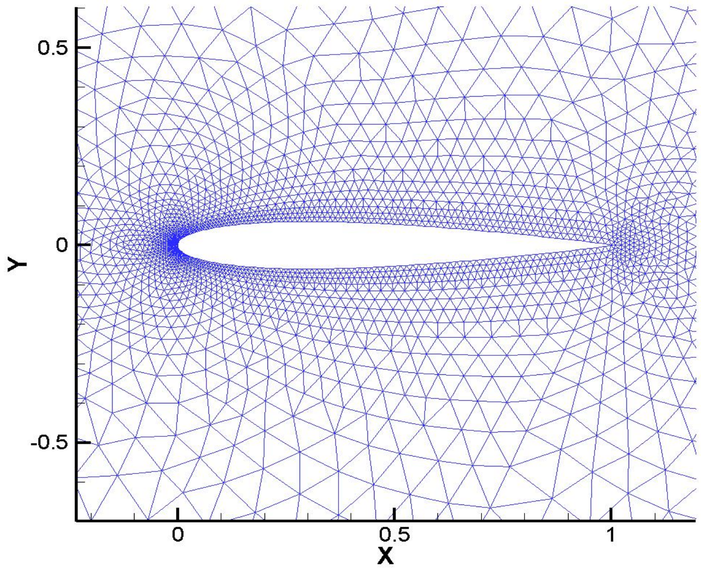

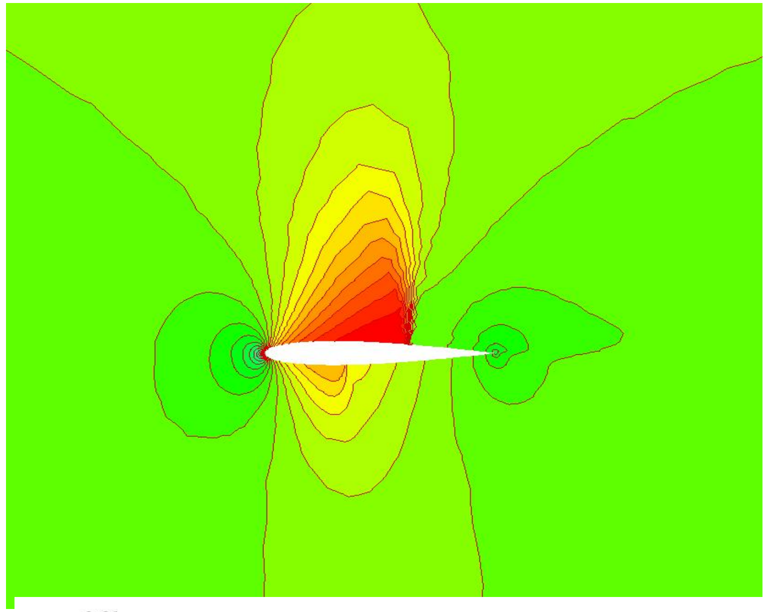

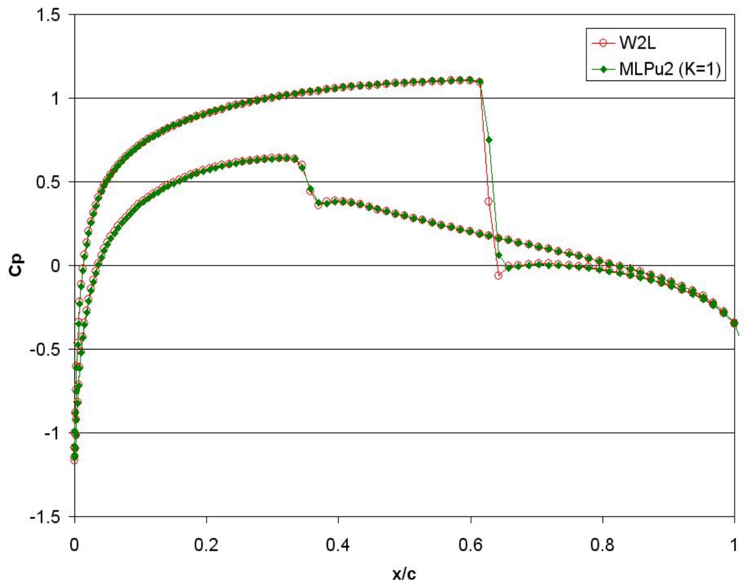

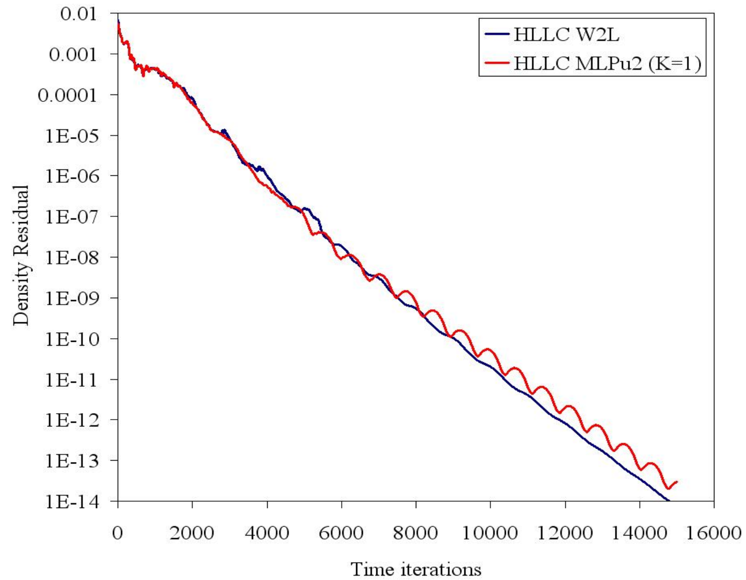

CONCLUSIONS

- In the FV approach different behavior is exhibited for grids where the center of the face does not coincide with the reconstruction location.

CONCLUSIONS

- In the FV approach different behavior is exhibited for grids where the center of the face does not coincide with the reconstruction location.
  - The proposed correction for the reconstruction values remedies the problem (for both the compact and wide stencil G-G gradient computations)

CONCLUSIONS

- In the FV approach different behavior is exhibited for grids where the center of the face does not coincide with the reconstruction location.
  - The proposed correction for the reconstruction values remedies the problem (for both the compact and wide stencil G-G gradient computations)
  - For the wide stencil similar consistent convergence behavior for all grid types is achieved along with improvements in accuracy

CONCLUSIONS

- In the FV approach different behavior is exhibited for grids where the center of the face does not coincide with the reconstruction location.

  - The proposed correction for the reconstruction values remedies the problem (for both the compact and wide stencil G-G gradient computations)
  - For the wide stencil similar consistent convergence behavior for all grid types is achieved along with improvements in accuracy
  - Convergence to steady-state solutions is greatly improved.

CONCLUSIONS

- In the FV approach different behavior is exhibited for grids where the center of the face does not coincide with the reconstruction location.

  - The proposed correction for the reconstruction values remedies the problem (for both the compact and wide stencil G-G gradient computations)
  - For the wide stencil similar consistent convergence behavior for all grid types is achieved along with improvements in accuracy
  - Convergence to steady-state solutions is greatly improved.
  - Accurate shock/bore computations can be obtained on all grid types

CONCLUSIONS

- In the FV approach different behavior is exhibited for grids where the center of the face does not coincide with the reconstruction location.
  - The proposed correction for the reconstruction values remedies the problem (for both the compact and wide stencil G-G gradient computations)
  - For the wide stencil similar consistent convergence behavior for all grid types is achieved along with improvements in accuracy
  - Convergence to steady-state solutions is greatly improved.
  - Accurate shock/bore computations can be obtained on all grid types
- The effect of the grid's geometry at the boundary can lead to order reduction for CCFV schemes, even for good quality grids

CONCLUSIONS

- In the FV approach different behavior is exhibited for grids where the center of the face does not coincide with the reconstruction location.
  - The proposed correction for the reconstruction values remedies the problem (for both the compact and wide stencil G-G gradient computations)
  - For the wide stencil similar consistent convergence behavior for all grid types is achieved along with improvements in accuracy
  - Convergence to steady-state solutions is greatly improved.
  - Accurate shock/bore computations can be obtained on all grid types
- The effect of the grid's geometry at the boundary can lead to order reduction for CCFV schemes, even for good quality grids
- Comparison using truly multidimensional limiting methods produced more consistent and accurate results

CONCLUSIONS

- In the FV approach different behavior is exhibited for grids where the center of the face does not coincide with the reconstruction location.
  - The proposed correction for the reconstruction values remedies the problem (for both the compact and wide stencil G-G gradient computations)
  - For the wide stencil similar consistent convergence behavior for all grid types is achieved along with improvements in accuracy
  - Convergence to steady-state solutions is greatly improved.
  - Accurate shock/bore computations can be obtained on all grid types
- The effect of the grid's geometry at the boundary can lead to order reduction for CCFV schemes, even for good quality grids
- Comparison using truly multidimensional limiting methods produced more consistent and accurate results
- The proposed approach depends mostly on the mesh characteristics and is independent on the Riemann solver used.

CONCLUSIONS

- In the FV approach different behavior is exhibited for grids where the center of the face does not coincide with the reconstruction location.
  - The proposed correction for the reconstruction values remedies the problem (for both the compact and wide stencil G-G gradient computations)
  - For the wide stencil similar consistent convergence behavior for all grid types is achieved along with improvements in accuracy
  - Convergence to steady-state solutions is greatly improved.
  - Accurate shock/bore computations can be obtained on all grid types
- The effect of the grid's geometry at the boundary can lead to order reduction for CCFV schemes, even for good quality grids
- Comparison using truly multidimensional limiting methods produced more consistent and accurate results
- The proposed approach depends mostly on the mesh characteristics and is independent on the Riemann solver used.
- Using an edge-based structure the method can be applied, relatively straight forward, to existing 2D FV codes.

Some References

- A.I.D., I.K. Nikolos and M.Kazolea, "Performance and comparison of cell-centered and node-centered unstructured finite volume discretizations for shallow water free surface flows", `Archives of Computational Methods in Engineering`, 18(1), p. 1-62, 2011
- A.I.D. and I.K. Nikolos, "A novel multidimensional solution reconstruction and edge-based limiting procedure for unstructured cell-centered finite volumes with application to shallow water dynamics", `International J. for Numerical Methods in Fluids` (in press), 2012.
- I.K. Nikolos and A.I.D., "Solution reconstruction and limiting for unstructured finite volumes: application to the Euler equations", (in preparation),

THANK YOU FOR YOUR ATTENTION!